INFLUENCE OF SMALL AMOUNTS OF NIOBIUM ON MECHANICAL AND CORROSION PROPERTIES OF TYPE 304 STAINLESS STEEL*

V. K. Sikka, A. J. Moorhead, and C. R. Brinkman
Metals and Ceramics Division
Oak Ridge National Laboratory
Oak Ridge, Tennessee 37830

ABSTRACT

Creep and creep-rupture properties of several experimental heats of type 304 stainless steel containing 20, 50, 100, 200, 500, 700, and 1000 ppm (by weight) of Nb were investigated in the temperature range of 482 to 649°C. Resistance to intergranular corrosion of these heats was also studied. Results of tests on the experimental heats were compared with the creep properties of 20 commercial heats of type 304 stainless steel and data from the literature on several heats of type 347 (4000 to 8000 ppm Nb) stainless steel.

Results on experimental heats were used to check that heat-to-heat variations in creep properties of 20 commercial heats of type 304 stainless steel are caused by variations in C, N, grain size, and for the most part by residual Nb (10 to 200 ppm). The time to rupture increased and minimum creep rate decreased with increasing Nb content until a saturation level was attained at about 500-1000 ppm.

Type 304 stainless steel containing 500 ppm Nb offers superior creep and creep-rupture properties with improved creep ductility and a factor of approximately 5 better intergranular corrosion resistance (in boiling $CuSo_4$ solution) than type 304 stainless steel (20 ppm Nb). In their welding work on the same heats, Moorhead et al. have observed that type 304 containing 500-1000 ppm Nb shows welding properties similar to that of type 304 stainless steel.

---

*Research sponsored by the Division of Reactor Research and Technology of the Department of Energy under contract W-7405-eng-26 with the Union Carbide Corporation.

DISCLAIMER

I. Introduction

Austenitic stainless steels of types 304 and 316 are the currently accepted structural material for breeder reactors. These steels are purchased to ASTM specifications. The range of allowable chemistry and thermo-mechanical processing history permitted by applicable material procurement specifications results in considerable variation in certain resultant mechanical properties[1-6]. It is the purpose of this paper to show the following:

1. Commercial heats exhibit variations in time to rupture (t_r) and minimum creep rate ($\dot{\varepsilon}_m$),
2. Whereas carbon and nitrogen variations are known to be responsible for significant variations in mechanical behavior, niobium content was also a major factor as determined from studies conducted on twenty commercial heats of type 304 stainless steel,
3. Time to rupture (t_r) as measured from uniaxial creep tests increases with increasing Nb up to 500-700 ppm and saturates beyond this range,
4. Type 304 stainless steel containing 500 ppm Nb offers creep-rupture properties comparable with types 316 and 347 stainless steels, but with improved ductility, and
5. Type 304 containing 500 ppm Nb is an optimum composition for improved creep and creep-rupture properties and intergranular attack in $CuSO_4$ solution. The work of Moorhead et al.[7] on the same heats has shown little effect on the weldability of type 304 containing 500 ppm Nb as compared to type 304.

II. Materials and Testing Procedures

II.1. Materials: Twenty commercial heats were used to study heat-to-heat variations, all of which were air-melted. These heats included 17 procured as plate, three as bar, and one as a 710 × 9.5-mm seamless pipe. The

details of heat numbers, vendor, product form, and grain size of twenty heats are presented in Table 1 and their chemical compositions are summarized in Table 2.

One group of experimental heats (used to explain heat-to-heat variations in commercial heats) contained Nb in the range of 20 to 200 ppm (by weight). Experimental heats with Nb contents of 500, 700, and 1000 ppm were made to determine an optimum composition yielding improved creep properties as compared to type 304 stainless steel and the niobium-stabilized type 347 stainless steel (Nb $\geq$ 10 $\times$ C).

The experimental heats were made by remelting one of the commercial heats (heat 187 containing 20 ppm Nb, Table 1 and 2) and adding niobium to reach final levels of 50, 100, 200, 500, 700, and 1000 ppm. These heats were made by melting the commercial heat in a water-cooled copper mold and remelting six times with a nonconsumable tungsten electrode in an evacuated chamber backfilled with partial pressure of argon. The final melt was drop cast into a 19-mm diameter water-cooled copper mold. The drop casts were preheated at 1000°C and hot swaged into 10-mm diameter rods, which were used in machining tensile and creep specimens. The chemical analyses of experimental heats are summarized in Table 3.

II.2. Test Specimens: The test specimens for commercial and the experimental heats were threaded-end bars having a gage diameter of 6.35-mm and a reduced section of 31.8-mm. In a few instances a larger specimen having a 57.2-mm reduced section was used for the commercial heats. All specimens were lathe machined. The machined specimens were inspected, cleaned, and those to receive additional heat treatment were reannealed at 1065°C for 0.5 hr in argon. The commercial heats were tested in both the as-received (mill-annealed) and reannealed (laboratory annealed) conditions, whereas experimental heats were only tested in

the reannealed condition. All experimental heats were tested after annealing for 0.5 hr at 1065°C. However, some heats were also tested after reannealing for 0.5 hr at 1093, 1150, and 1250°C. The grain sizes for both the commercial and experimental heats were measured and are summarized in Tables 1 and 3, respectively.

II.3. Testing Procedures: The creep tests were performed according to ASTM specification[8] E 139-70. The stress-rupture tests were conducted in standard lever-arm creep machines calibrated to a load accuracy of $\pm$0.5 percent. The temperature was measured by three Chromel versus Alumel thermocouples (of wire accuracy of $\pm$3/8 percent) wired to the specimen. The temperature variation along the specimen gage length was approximately $\pm$1°C, and the highest temperature was taken as the nominal test temperature.

Length changes were measured by extensometers attached by set-screws to small grooves in the specimen shoulders. The extensometer movement was read by both dial gages and averaging transducers. The dial gages and tranducers had an accuracy of ±2.5μm. The specimen shoulder effects were negligible as compared to overall creep elongation.

III. Results and Discussion

III.1. Time to Rupture (t_r) and Minimum Creep Rate ($\dot{\varepsilon}_m$):

III.1.1. Heat-to-Heat Variations: Time to rupture data at 593°C on 20 heats of type 304 stainless steel are plotted as a function of stress in Fig. 1. These data are on materials in both mill-annealed and laboratory annealed conditions. Minimum creep rate data on the same heats are plotted in Fig. 2. Figure 1 shows that time to rupture can vary by factors of 30-40 for 20 heats in both the mill-annealed and laboratory annealed conditions. Heat-to-heat variations observed for short-term data are also becoming obvious in long-term

data extending to test times beyond 50,000 hr. Figure 2 shows that minimum creep rate can vary by factors of 100 for the same heats. This is apparent for both the short-term and long-term creep data.

The stress exponent, n_r, ($t_r = A\sigma^{-n_r}$) for rupture data on various heats varied from 8.2 to 14.5 for weak to the strong heats, respectively. The stress exponent, n_m, for $\dot{\varepsilon}_m$ ($\dot{\varepsilon}_m = B\sigma^{n_m}$) ranged from 9.6 to 16.5 for the same heats. In general, the stress exponents n_r and n_m were low for the weak heats and high for the strong heats.

III.1.2. Correlations Between Heat-to-Heat Variations and Chemical Composition: A summary[9] of several studies has shown that t_r increases and $\dot{\varepsilon}_m$ decreases with increasing amounts of carbon and nitrogen (C+N). Thus, t_r and $\dot{\varepsilon}_m$ data on 20 heats at 593°C and 207 MPa were plotted as a function of (C+N) in Figs. 3(a) and 4(a). These figures show that the heats containing the highest (C+N) have a higher time to rupture and a lower minimum creep rate as compared to heats of lower (C+N) levels. However, data scatter is too great to observe any definite trends. The same data, when plotted as a function of $(C+N)/\sqrt{d}$ [Figs. 3(b) and 4(b)] shows that grain size, d, plays an important role in heat-to-heat variations. These figures still show the separation of data into two bands showing the general trend of increasing t_r and decreasing $\dot{\varepsilon}_m$ with an increase in $(C+D)/\sqrt{d}$. Figures 3(c) and 4(c) show that the data in two bands can be combined by plotting it against $(C+N + 10Nb)/\sqrt{d}$. Figures 3(c) and 4(c) show that the data in two bands can be combined by plotting it against $(C+N + 10Nb)/\sqrt{d}$.

The correlation coefficient R^2 for t_r improved from 31.31 to 65.9% in going from (C+N)$/\sqrt{d}$ to (C+N + 10Nb)$/\sqrt{d}$. Similar improvement in $\dot{\varepsilon}_m$ correlations was from 35.50 to 78.03%. A correlation coefficient of 100% describes the data perfectly. A multiplication factor of 10 required to account for niobium effects indicated that niobium is probably a more potent strengthener than C, N, and the small grain size. In order to check this hypothesis we have plotted t_r and $\dot{\varepsilon}_m$ as a function of Nb content in Figs. 3(d) and 4(d). The correlation coefficients for least square analysis to these plots were 57.53 and 61.0%, respectively. The filled and half-filled symbols are for commercial heats with rather high nitrogen content (0.14%); heat 121, and large grain size (280 m), heat 796, respectively, and therefore they are described better by (C+N + 10Nb)$/\sqrt{d}$ relationship [Figs. 3(c) and 4(c)]. A comparison of correlation coefficients for various chemical composition and grain size parameters indicated that although a complex relationship like (C+N + 10Nb)$/\sqrt{d}$ best describes the data, a single term like niobium content can describe most of the heat-to-heat variations in creep data on 20 heats of type 304 stainless steel.

III.1.3. Experimental Versus Commercial Heats: In order to confirm the importance of Nb in heat-to-heat variations, we remelted heat 187 which originally contained 20 ppm Nb and made several experimental heats containing 20 (remelted condition), 50, 100, 200, 500, 700, and 1000 ppm Nb. Heats containing 20, 50, 100, 200, and 500 ppm Nb were made during the first melt. A second melt was used to make 20, 500, 700, and 1000 ppm heats. Since the first and second melt were slightly different in properties, their data have been identified separately.

Creep tests on the experimental heats were performed at 482, 538, 593, and 649°C and the results are summarized in Table 4. Results obtained from experimental and commercial heats are compared in Figs. 5 and 6. These data show a good correlation between creep behavior and Nb content for both experimental and commercial heats and confirm the findings in Section III.1.2 that variation in niobium content is an important factor in explaining heat-to-heat variations.

III.1.4. Comparisons Between Experimental Heats of Type 304 Stainless Steel and Commercial Heats of Type 347 Stainless Steel: Figures 5 and 6 also include data[10] on commercially available Nb-stabilized type 347 stainless steel. This steel contains Nb $\geq$ 10 C by weight percent, which is 1000 times greater than that in the weakest heat of type 304 and a factor of 10 greater than in the highest niobium containing experimental heats. These figures show that t_r does not increase monotonically with increasing Nb, but shows a saturation effect beyond 500–1000 ppm Nb. Thus, increasing Nb to levels used in type 347 stainless steel produces no additional improvement in creep properties. However, type 347 stainless steels with the high niobium content were originally developed for improved resistance to intergranular corrosion attack.

III.1.5. Heat Treatment Effects on Creep Properties of Experimental Heats: Both commercial and experimental heats were annealed for 0.5 hr at 1065°C prior to creep testing in the reannealed condition. However, experimental heats containing 20, 500, and 1000 ppm Nb were also annealed for 0.5 hr at 1150°C to check their response to heat treatment temperature. Results of these tests are included in Table 4, which show that the higher annealing treatment produces slightly lower creep rates with improved rupture life. Thus, experimental heats containing varying amounts of Nb appear stable to high heat treatment temperatures.

III.1.6. Comparison of Experimental Heat Behavior with that of Commercial Heats of Type 304 and 316 Stainless Steel: Figure 7(a) shows a comparison of rupture data obtained from the experimental niobium-containing heats with upper and lower statistical defined data bounds observed for type 304 stainless steel. These bounds were developed by Sikka and Booker[11] on the creep data collected from various sources in the United States. The upper and lower bounds represent expected ±2 standard error of estimates (SEE) in log t_r. Figure 7(b) shows a similar comparison with the upper and lower bound observed for type 316 stainless steel. For the sake of clarity, this figure only includes data on 20, 500, 700, and 1000 ppm Nb heats. From Fig. 7(a) we can see that while the 20 ppm heat falls close to the lower bound, heats containing 500 ppm and higher Nb fall close to the upper bound for type 304 stainless steel. Figure 7(b) shows that the 500 ppm and higher Nb heats also fall above average or closer to the upper bound for type 316 stainless steel. Figures 5(a) and 6(a) have already shown that experimental heats containing 500–1000 ppm Nb heats have creep and creep-rupture properties similar to those of type 347, which contains Nb = 10 C. Thus, we have observed from the experimental heats that variations in Nb content at small concentration levels can result in substantial heat-to-heat variations in creep response, but increasing the Nb content improved results in creep and creep-rupture properties of type 304 stainless steel.

III.2. Creep Properties at Low Temperatures: Creep and creep-rupture properties have thus far been described only at high temperatures of 593 and 649°C. However, these steels may have to operate in many instances between 427 and 538°C if used in breeder reactor applications. Thus, a few creep tests were performed at 482 and 538°C and their results are shown in Figs. 8(a) and (b). The creep curves in these figures clearly show a significant improvement in creep resistance of steels containing 500 ppm and higher Nb content even at low test temperatures. Thus, small additions of Nb not only improve creep and creep-rupture properties at high temperatures but also at low temperatures as well.

III.3. Creep Time (t_s) and Strain (e_s) to Onset of Tertiary Creep: These properties are plotted as a function of Nb content in Figs. 9 and 10. These figures show that t_s increases with increasing Nb, while e_s decreases and also that there is excellent agreement between the commercial and experimental heats with respect to behavior based on niobium content. The increase in t_s with increasing Nb content suggests that the improved properties of Nb containing steels are not only derived from delaying the rupture process, but also the overall creep deformation process.

In a previous paper Booker and Sikka[12] have shown that t_s is related to by

$$t_s = 0.752 t_r^{0.977} . \quad (1)$$

Equation (1) is valid over a temperature range of 482 to 816°C. Figure 11 shows a comparison of data on experimental heats with the average and upper and lower bounds derived from Eq. 1. This figure shows that the data on experimental heats are still within the upper and lower bounds, but on the lower side for the higher Nb heats, which suggests that t_s may be a lower fraction of t_r for these heats as compared to type 304 stainless steel. However, the results in Figs. 9(a) and 10(a) have shown that besides being a lower fraction of t_r, t_s still increases with increasing Nb content. Thus, it can be concluded that increasing Nb content of type 304 stainless steel does not cause any premature occurrence of the onset of tertiary creep.

III.4. Creep-Rupture Ductility: Figures 12(a) and (b) show total creep elongation for the experimental Nb containing heats and for type 347 stainless steel compared with the upper and lower bound[11] for type 304 stainless steel. These figures show that total elongation values of type 347 heats fall below the lower bound for type 304 and even reach values as low as 1%. However, total elongation values for the experimental Nb containing heats fall close to the upper bound.

III.5. Correlation Between Tensile and Creep Properties: Tensile tests were performed on the experimental heats (Table 5) at the creep test temperature to check the validity of previously developed[13] models of t_r and $\dot{\varepsilon}_m$ containing

elevated temperature ultimate tensile strength (U) terms, which are given by

$$\log t_r = 5.716 - 3915 \frac{\log \sigma}{T} + 32.60 \frac{U}{T} - 0.007303\ U \log \sigma\ , \qquad (2)$$

$$\log \dot{\varepsilon}_m = 2.765 + 3346 \frac{\log \sigma}{T} - 51.83 \frac{U}{T} + 0.01616\ U \log \sigma\ , \qquad (3)$$

for σ and U in MPa and T in K.

The predicted values from Eqs. 2 and 3 are compared with the data on experimental Nb containing heats in Figs. 13 and 14. These figures show excellent agreement between the predicted and the experimental values. Furthermore, they provide additional support as to the applicability of previously published[12] relationships between tensile and creep properties in predicting the creep properties of newly developed experimental heats of essentially type 304 stainless steel.

The use of U in predicting creep properties of experimental heats (Figs. 13 and 14) and the correlation between the creep properties of Nb content (Figs. 5 and 6) require that U and Nb concentration be related. This is shown in Fig. 15. Although there is considerable scatter (possibly due to other factors discussed by Booker and Sikka[5]) the trend is evident that U increases with increasing Nb content. Furthermore, U values on experimental heats from the first melt show excellent agreement with the data on commercial heats. Reasons for higher values of U observed for experimental heats from the second melt [Figs. 15(a) and (b)] are not clear, but the effect of these values were reflected in the creep properties.

III.6. Strauss Test and Hot-Cracking Results: Niobium is added to stabilized type 347 stainless steel to improve its resistance to intergranular attack. However, this steel suffers from cracking[14] in the heat-affected zone on welding thick sections. Thus, when experimental heats are developed, an optimum Nb yielding improved creep properties should consider the following points:

1. Too little Nb may yield poor intergranular corrosion resistance properties depending upon the intended application, and
2. Too much Nb may produce cracking in the heat-affected zone on welding thick sections.

Strauss[15] tests were performed on experimental heats with varying Nb content, a commercial heat of type 304 containing 200 ppm Nb, and a commercial heat of type 347 stainless steel. All heats were sensitized for 0.5 hr at 677°C. Photomicrographs of the U-bend test specimens and the microstructure taken in the maximum tensile stress region of the U-bends are shown in Fig. 16. The extent of intergranular attack was measured by crack facet length (CFL), which was defined as

$$CFL = n \cdot d \qquad (4)$$

where

n = number of cracked facets per unit area, and

d = facet length ≈ 1/2 average grain intercept.

The CFL values were calculated from micrographs in Fig. 16 and are plotted as a function of Nb content in Fig. 17. This figure shows that CFL drops sharply with increasing Nb contents and its values for 500 ppm heat are only 20 percent of those observed for type 304.

Moorhead et al.[7] performed welding tests using a Tigma Jig machine on experimental heats with varying niobium content. They showed that heats containing 500 to 1000 ppm Nb were similar in welding behavior to type 304 in that they retained resistance to cracking in the heat-affected zone as compared to extensive cracking observed in type 347 for the same test conditions. Details of welding procedure and data analysis are available in the paper by Moorhead et al.[7]

III.7. Optical and Transmission Electron Microscopy:

Optical micrographs for creep specimens tested at 649°C and 172 MPa are shown in Figs. 18 and 19. Micrographs in Fig. 18 are for specimens taken from first melt and those in Fig. 19 are for specimens taken from second melt. Microstructures in Figs. 18 and 19 are specimens annealed for 0.5 hr at 1065°C prior to creep testing. Figure 20 compares micrographs for specimens annealed for 0.5 hr at 1150°C. All specimens showed extensive intragranular deformation.

Some intergranular cavitation was observed, but fracture appeared to be transgranular. Grain sizes for melt one and two showed no significant difference (Figs. 18 and 19). The grain sizes of 20 and 500 ppm heats were essentially the same even after annealing at 1150°C. However, the grain size for the 1150°C anneal was coarser than 1065°C anneal.

Transmission electron photomicrographs of the annealed specimens of experimental Nb containing heats and for type 347 steel are shown in Fig. 21. Precipitates were observed in all heats containing Nb. However, these precipitates were semi-coherent (showed no electron diffraction spots) for Nb content less than 1000 ppm and incoherent for the higher niobium levels. The incoherent precipitates were identified as NbC type. Most of the precipitates were in the matrix while the grain boundaries were clean. It is probably these precipitates which impart improved creep and other properties by either modifying size, shape, and distribution of $M_{23}C_6$ or changing relative nucleation and growth of these precipitates at grain boundaries and in the matrix.

SUMMARY AND CONCLUSIONS

Large heat-to-heat variations in creep and creep-rupture properties were observed for 20 commercial heats of type 304 stainless steel. Although these variations were best correlated by the relationship (C+N + 10 Nb)/$\sqrt{d}$, niobium alone could account for most variations with the exception of a high nitrogen heat (121) and a coarse grain heat (796). Experimental heats confirmed the importance of small niobium content in causing heat-to-heat variations in commercial heats of type 304 stainless steel. The following are some important conclusions from this work:

1. Time to rupture (t_r) for commercial and experimental heats increased and minimum creep rate ($\dot{\varepsilon}_m$) decreased with increasing Nb content and these

properties saturated beyond 500–1000 ppm to the 10^4 ppm level. The saturated values of t_r were higher for high (C+N) content and fine grain material.

2. Experimental heats of type 304 stainless steel containing 500 ppm Nb resulted in improved creep and creep-rupture properties at both low (482 and 538°C) and high temperatures (593 and 649°C) investigated.
3. Creep-rupture times and minimum creep rate behavior for experimental heats of varying niobium content could be estimated from a knowledge of their elevated temperature ultimate tensile strength values.
4. The creep-rupture strength for experimental heats of type 304 stainless steel containing 500 ppm Nb were comparable to that of type 347 stainless steel, but with significantly higher ductility.
5. Type 304 stainless steel containing 500 ppm Nb offers superior creep and creep-rupture prperties with improved ductility, a factor of approximately 5 better corrosion resistance, and still retains welding response similar to type 304 stainless steel (Moorheat et al.[7]). It should be noted, however, that the effect of Nb on the creep-rupture properties of type 304 stainless steel weldments is unknown.

REFERENCES

1. V. K. Sikka, H. E. McCoy, M. K. Booker, and C. R. Brinkman, *Journal of Pressure Vessel and Technology*, Vol. 97, 1975, pp. 243-251.
2. H. E. McCoy, *Tensile and Creep Properties of Several Heats of Type 304 Stainless Steel*, ORNL/TM-4709, Oak Ridge National Laboratory, Oak Ridge, Tennessee, November 1974.
3. C. R. Brinkman and G. E. Korth, *Journal of Nuclear Technology*, Vol. 48, 1973, pp. 293-306.
4. D. R. Diercks and D. T. Raske, *Elevated Temperature Strain Controlled Fatigue Data of Type 304 Stainless Steel — A Compilation, Multiple Linear Regression Model and Statistical Analysis*, ANL-76-95, Argonne National Laboratory, 1976.
5. M. K. Booker and V. K. Sikka, "Effect of Composition Variables on the Tensile Properties of Type 304 Stainless Steel," to be published as a part of the ASTM Symposium on The Effect of Carbon, Nitrogen, and Residual Elements on the Austenitic Stainless Steels and Their Weldments, November 14-15, 1977, in Atlanta, Georgia.
6. L. A. James, "The Effect of Heat-to-Heat Variations and Melt Practice Variations Upon Fatigue-Crack Growth in Two Austenitic Steels," to be published as a part of the ASTM Symposium on The Effect of Carbon, Nitrogen, and Residual Elements on the Austenitic Stainless Steels and Their Weldments, November 14-15, 1977, in Atlanta, Georgia.
7. A. J. Moorhead, V. K. Sikka, and R. W. Reed, "The Effect of Small Additions of Niobium on the Welding Behavior of an Austenitic Stainless Steel," to be published as a part of the ASTM Symposium on The Effect of Carbon, Nitrogen, and Residual Elements on the Austenitic Stainless Steels and Their Weldments, November 14-15, 1977, in Atlanta, Georgia.

8. "Recommended Practice for Conducting Creep, Creep-Rupture, and Stress-Rupture of Metallic Materials," Designation E 139-70, 1971, Annual book of ASTM Standards, Part 31, American Society for Testing and Materials, Philadelphia, 1971, pp. 470-483.

9. J. J. Heger and G. V. Smith, "Elevated Temperature Properties as Influenced by Nitrogen Additions to Types 304 and 316 Austenitic Stainless Steel," ASTM Special Technical Publication No. 522, American Society for Testing and Materials, Philadelphia, 1968.

10. W. F. Simmons and A. J. van Echo, "The Elevated Temperature Tensile Properties of Stainless Steel," ASTM Data Ser. D55S1, American Society for Testing and Materials, 1965.

11. V. K. Sikka and M. K. Booker, *Journal of Pressure Vessel Technology*, Vol. 99, 1977, pp. 298-313.

12. M. K. Booker and V. K. Sikka, *Nuclear Technology*, Vol. 30, 1976, pp. 52-64.

13. V. K. Sikka, M. K. Booker, and C. R. Brinkman, *Use of Ultimate Tensile Strength to Correlate and Estimate Creep and Creep-Rupture Behavior of Types 304 and 316 Stainless Steel*, ORNL-5285, Oak Ridge National Laboratory, October 1977.

14. D. A. Woodford and R. M. Goldhoff, *Material Science Engineering*, Vol. 5, 1969/70, pp. 303-324.

15. "Standard Recommended Practices for Detecting Susceptibility to Intergranular Attack in Stainless Steel," Designation A 262-70 (Practice E), Annual Book of Standards, Part 10, American Society of Testing and Materials, Philadelphia, 1976, pp. 1-27.

Acknowledgements

We gratefully acknowledge R. L. Hendricks for making the experimental heats, L. T. Ratcliff for performing tensile tests, R. H. Baldwin and C. O. Stevens for performing creep tests, J. C. Griess, Jr. for helping in corrosion testing, A. J. Moorhead for performing the welding tests, C. W. Houck for metallography, and H. Jang and J. Moteff (University of Cincinnati) for performing the transmission electron microscopy. We are also thankful to J. R. DiStefano and J. R. Keiser for reviewing, G. M. Slaughter and P. Patriarca for approving, and Linda Croff for typing the manuscript.

List of Figures

1. Heat-to-heat variations in time to rupture at 593°C for 20 commercial heats of type 304 stainless steel.

2. Heat-to-heat variations in minimum creep rate at 593°C for 20 commercial heats of type 304 stainless steel.

3. Plots of time to rupture (t_r) at 593°C and 207 MPa versus various chemical composition and grain size factors for 20 commercial heats of type 304 stainless steel. (a) t_r versus C + N, (b) t_r versus $C + N/\sqrt{d}$, (c) t_r versus $C + N + 10\ Nb/\sqrt{d}$, and (d) t_r versus Nb content. Curve in Fig. 3(c) is visual and was drawn to show the trends.

4. Plots of minimum creep rate ($\dot{\varepsilon}_m$) at 593°C and 207 MPa versus various chemical composition and grain size factors for 20 commercial heats of type 304 stainless steel. (a) $\dot{\varepsilon}_m$ versus (C + N), (b) $\dot{\varepsilon}_m$ versus $C + N/\sqrt{d}$, (c) $\dot{\varepsilon}_m$ versus $C + N + 10\ Nb/\sqrt{d}$, and (d) $\dot{\varepsilon}_m$ versus Nb content. Curve in Fig. 4(c) is visual and was drawn to show the trends.

5. Time to rupture as a function of Nb content for the commercial and experimental heats of type 304 stainless steel and commercial heats of type 347. (a) At 593°C and 207 MPa, and (b) at 649°C and 172 MPa. Bands in these plots are visual and were drawn to show the trends.

6. Minimum creep rate as a function of Nb content for the commercial and experimental heats of type 304 stainless steel and commercial heats of type 347. (a) At 593°C and 207 MPa, and (b) at 649°C and 172 MPa. Bands in these plots are visual and were drawn to show the trends.

7. Comparison of time to rupture data on Nb containing heats with upper and lower data scatter bounds for types 304 and 316 stainless steels at 593 and 649°C. (a) Type 304, (b) type 316.

8. Creep curves for experimental heats of type 304 stainless steel containing various amounts of Nb. (a) At 482 and 207 MPa, (b) at 538 and 276 MPa. Note the significant improvement in creep resistance for heats containing 500 ppm Nb.

9. Tertiary creep data as a function of Nb content for commercial and experimental heats of type 304 stainless steel at 593°C and 207 MPa. (a) Time to onset of tertiary creep, (b) strain to onset of tertiary creep.

10. Tertiary creep data as a function of Nb content for commercial and experimental heats of type 304 stainless steel at 649°C and 172 MPa. (a) Time to onset of tertiary creep, (b) strain to onset of tertiary creep.

11. Comparisons of time to onset of tertiary (t_s) creep data on experimental Nb heats with the average and upper and lower bounds of t_s versus t_r for type 304 stainless steel.

12. Comparison of creep total elongation data on experimental Nb heats and commercial heats of type 347 stainless steel with upper and lower bounds for type 304 stainless steel. (a) Experimental Nb heats, (b) type 347.

13. Plots of creep data on experimental niobium heats at 593°C and 207 MPa as a function of ultimate tensile strength at the creep test temperature. (a) Time to rupture, (b) minimum creep rate. Plots also include predicted curves from ORNL models containing an elevated temperature ultimate tensile strength term.

14. Plot of creep data on experimental niobium heats at 649°C and 172 MPa as a function of ultimate tensile strength at the creep test temperature. (a) Time to rupture, (b) minimum creep rate. Plots also include predicted curves from ORNL models containing an elevated temperature ultimate tensile strength term.

15. Plots of ultimate tensile strength as a function of Nb content for commercial and experimental heats of type 304 and commercial heats of type 347 stainless steel. (a) 593°C, (b) 649°C.

16. Micrographs showing improvement in intergranular resistance as a function of increasing Nb (20 to 1000 ppm) in experimental heats of type 304 stainless steel. For comparison, a micrograph on commercial heat of type 347 is also included.

17. Plot of crack facet length (CFL) as a function of Nb content for experimental heats of type 304 stainless steel and a commercial heat of type 347. The CFL values in this plot are from same size micrographs on each heat.

18. Micrographs showing fracture and edge near the fracture for specimens creep tested at 649°C and 172 MPa. (a) and (b) 20 ppm, (c) and (d) 50 ppm, (e) and (f) 200 ppm, (g) and (h) 500 ppm. All specimens were annealed at 1065°C for 0.5 hr prior to creep testing. Note that there are no significant differences between the fracture of specimens containing various niobium content.

19. Micrographs showing fracture and edge near the fracture for specimens creep tested at 649°C and 172 MPa. (a) and (b) 20 ppm, (c) and (d) 500 ppm, (e) and (f) 700 ppm, and (g) and (h) 1000 ppm. All specimens were from second melt and were annealed at 1065°C for 0.5 hr prior to creep testing. Note that there are no obvious microstructural differences between the first and second melt.

20. Micrographs showing fracture for specimens annealed at 1150°C for 0.5 hr and creep tested at 649°C and 172 MPa. (a) 20 ppm and (b) 500 ppm. The 1150°C annealed specimens had slightly coarser grain size than observed in Fig. 18 and 19 for the 1065°C annealed specimens.

21. Transmission electron micrographs for experimental heats of type 304 containing varying amounts of Nb and on a commercial heat of reannealed type 347 stainless steel. Note the difference in precipitation with increasing Nb content.

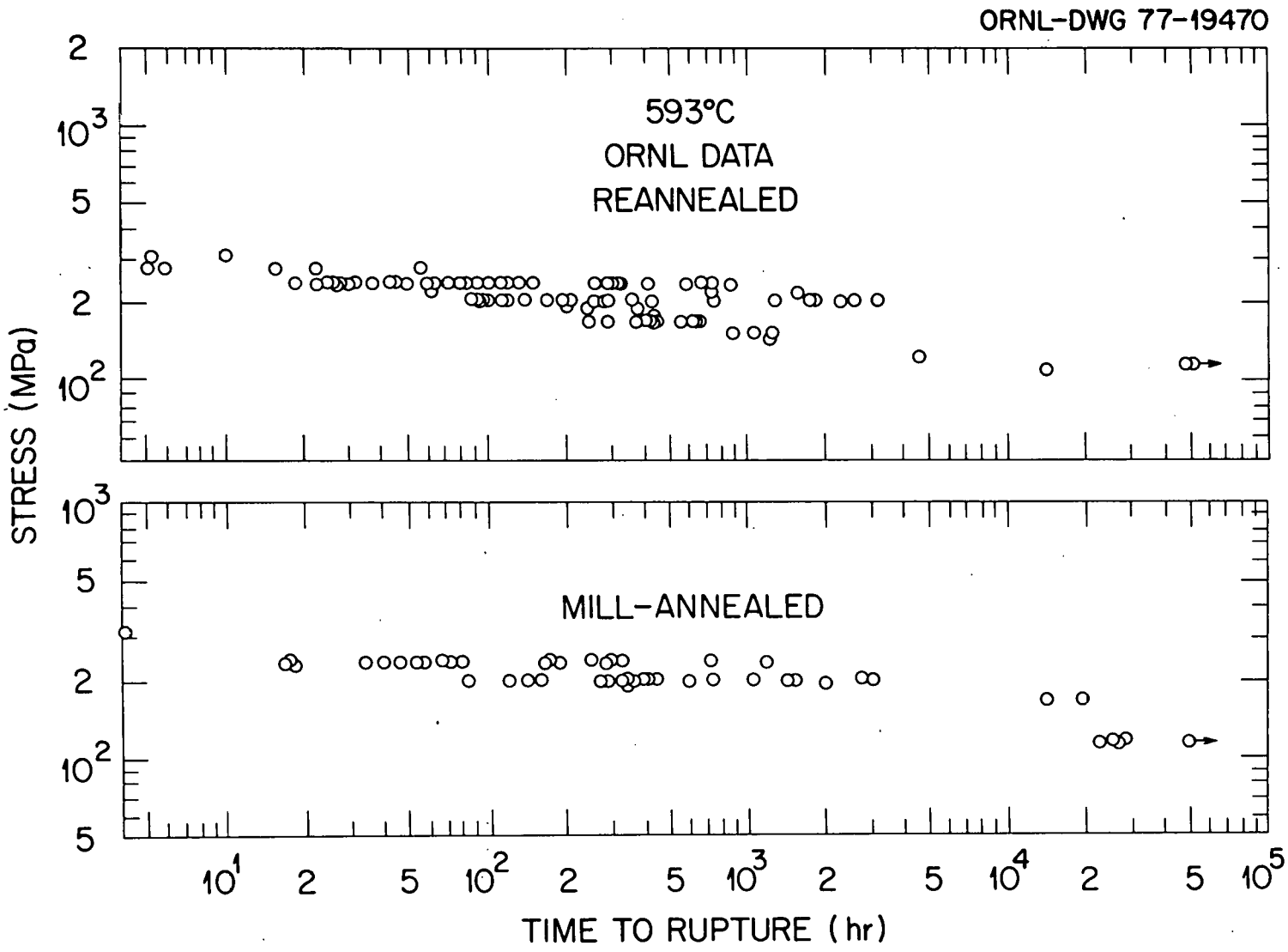

Fig. 1. Heat-to-heat variations in time to rupture at 593°C for 20 commercial heats of type 304 stainless steel.

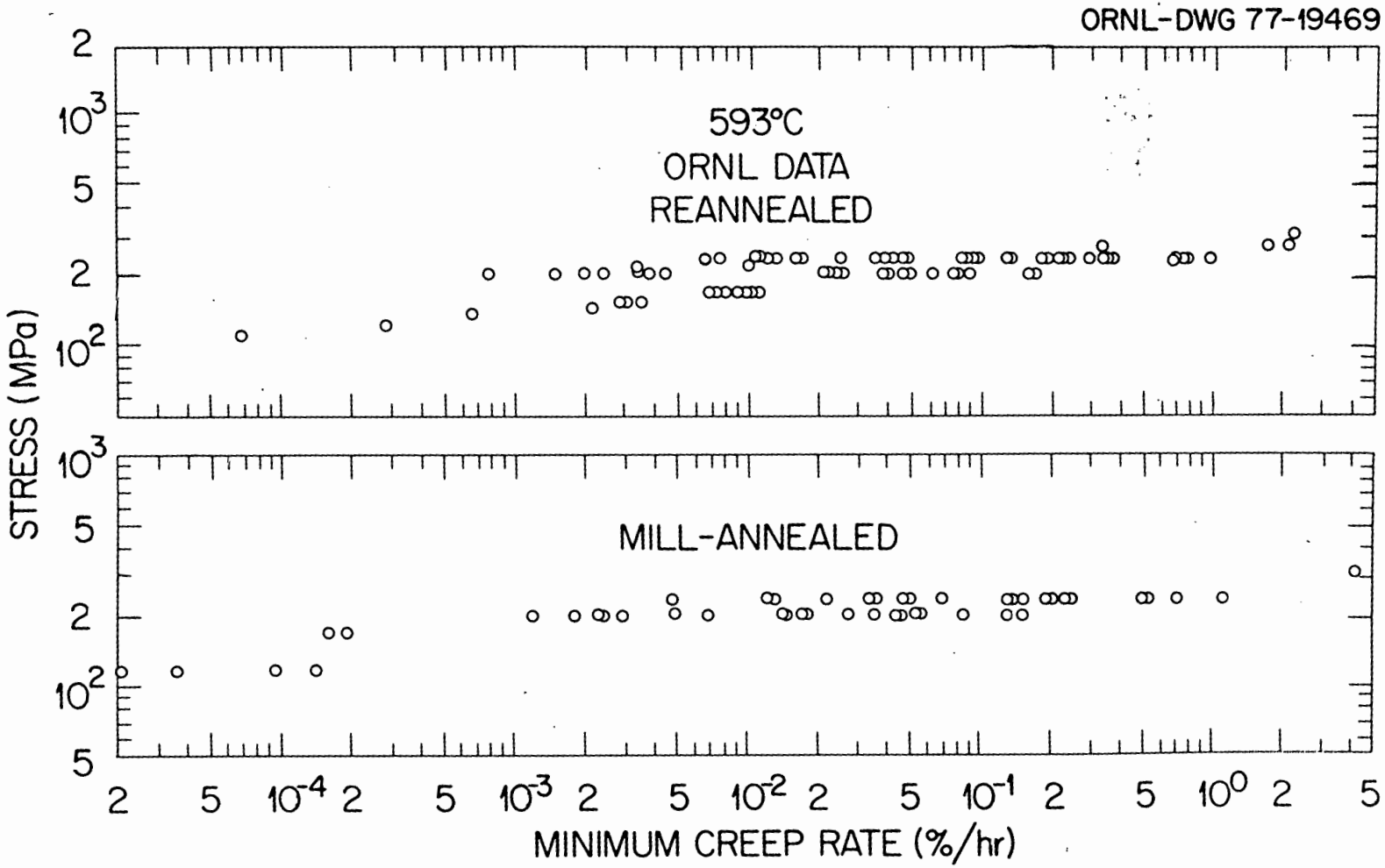

Fig. 2. Heat-to-heat variations in minimum creep rate at 593°C for 20 commercial heats of type 304 stainless steel.

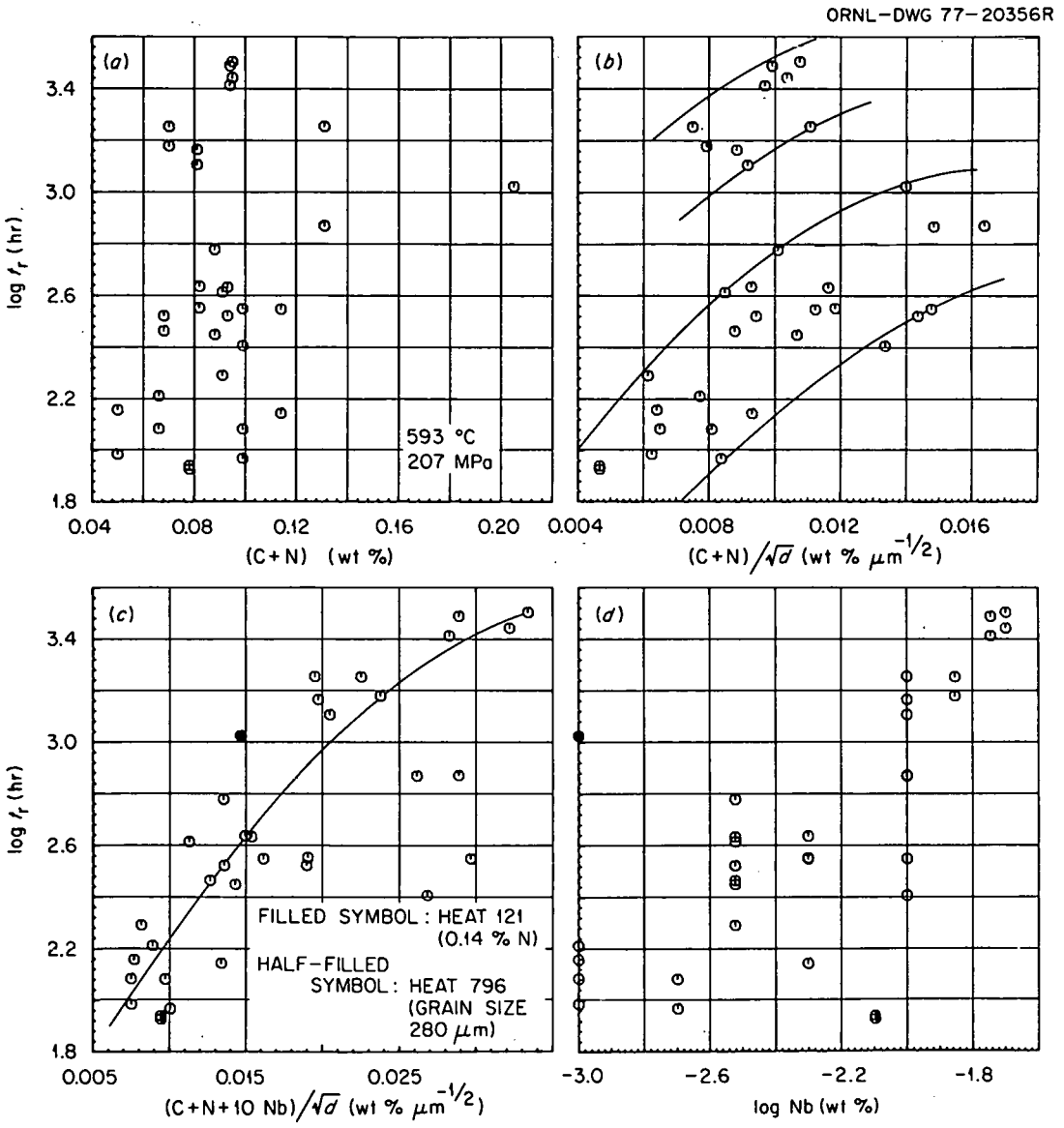

Fig. 3. Plots of time to rupture (t_r) at 593°C and 207 MPa versus various chemical composition and grain size factors for 20 commercial heats of type 304 stainless steel. (a) t_r versus C + N, (b) t_r versus C + N/$\sqrt{d}$, (c) t_r versus C + N + 10 Nb/$\sqrt{d}$, and (d) t_r versus Nb content. Bands in Fig. 3(c) are visual and were drawn to show the trends.

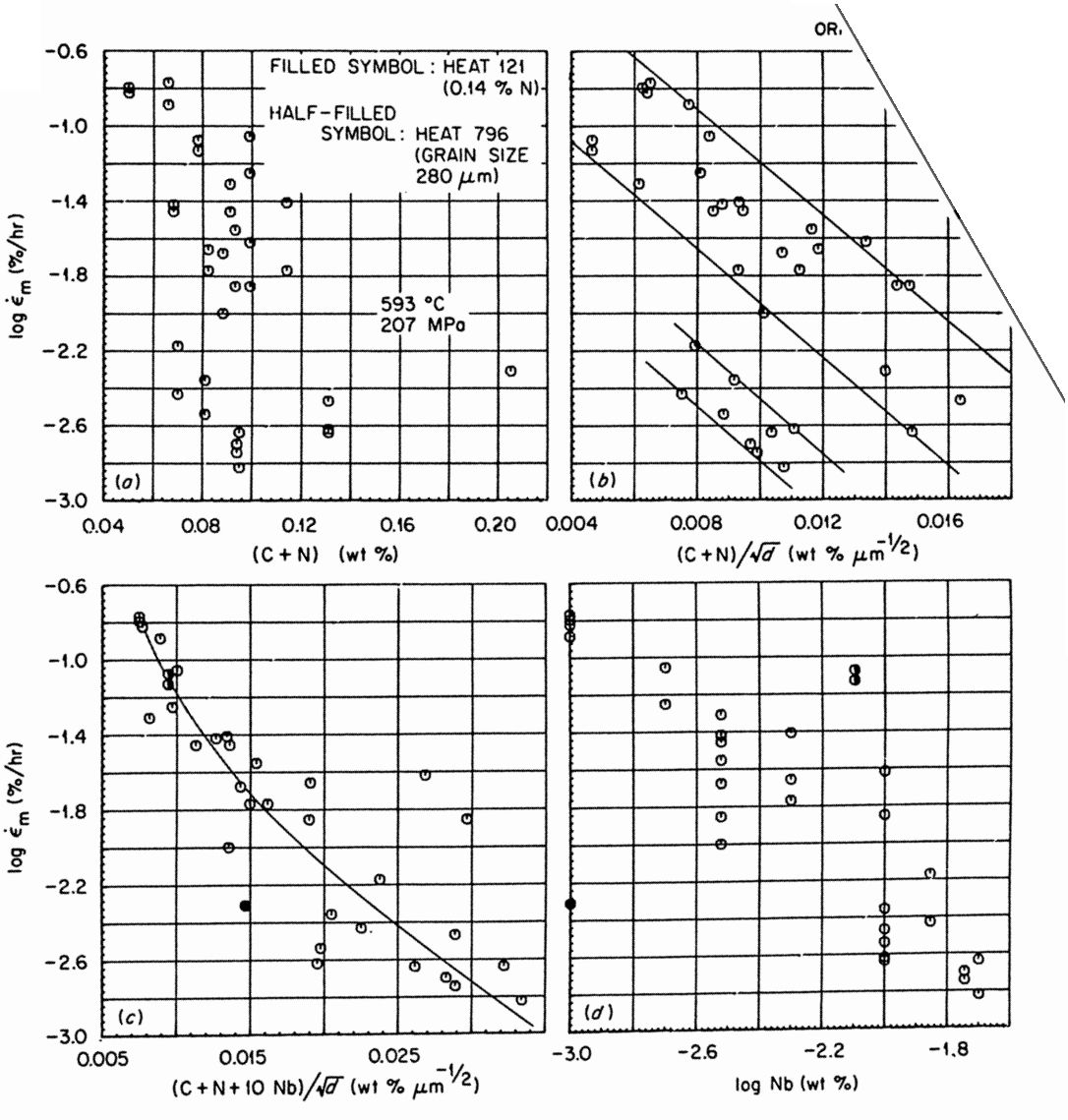

Fig. 4. Plots of minimum creep rate (ε_m) at 593°C and 207 MPa versus various chemical composition and grain size factors for 20 commercial heats of type 304 stainless steel. (a) $\dot{\varepsilon}_m$ versus (C + N), (b) $\dot{\varepsilon}_m$ versus C + N/$\sqrt{d}$, (c) $\dot{\varepsilon}_m$ versus C + N + 10 Nb/$\sqrt{d}$, and (d) ε_m versus Nb content. Bands in Fig. 4(c) are visual and were drawn to show the trends.

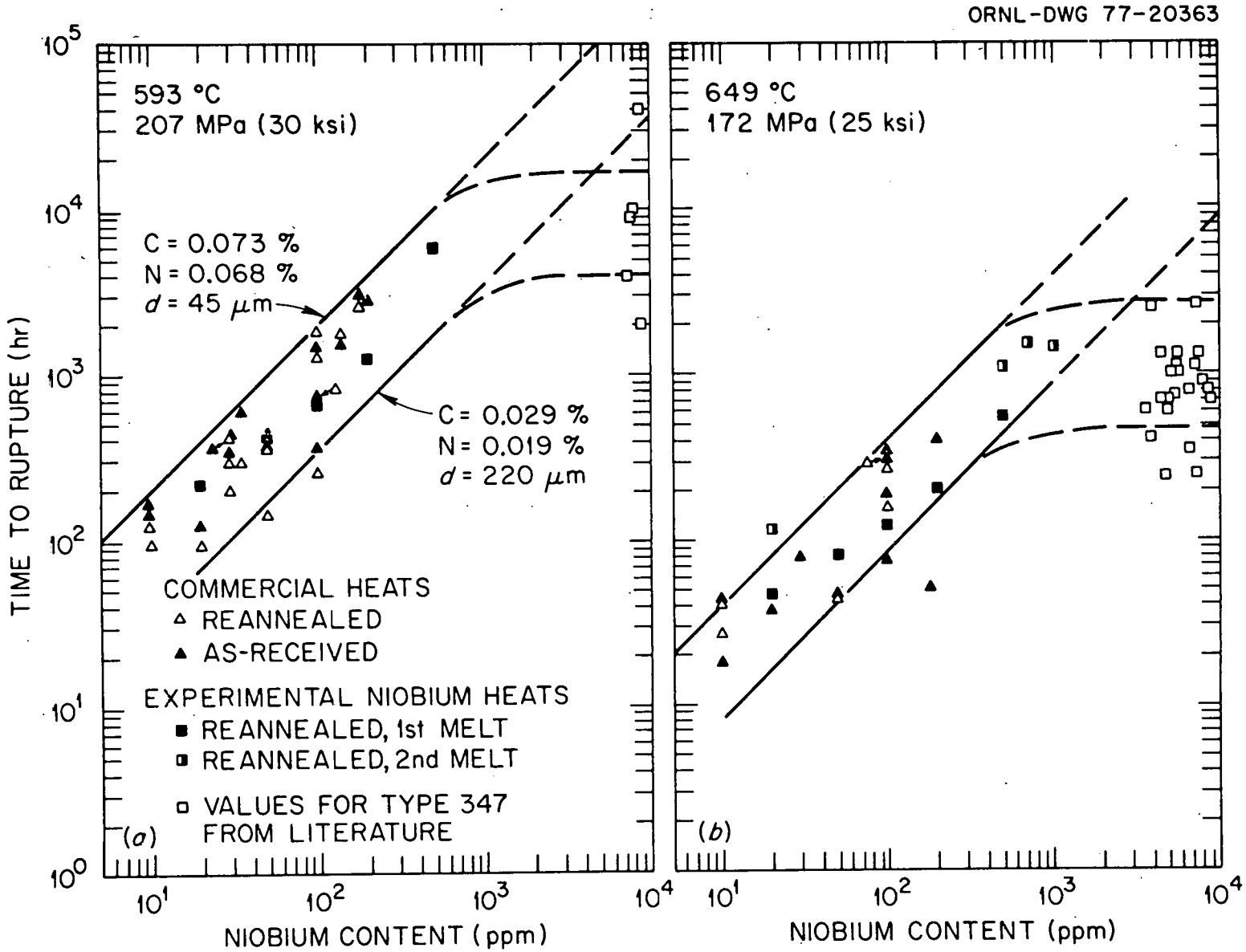

Fig. 5. Time to Rupture as a Function of Nb Content for the Commercial and Experimental Heats of Type 304 Stainless Steel and Commercial Heats of Type 347. (a) At 593°C and 207 MPa, and (b) at 649°C and 172 MPa. Bands in these plots are visual and were drawn to show the trends.

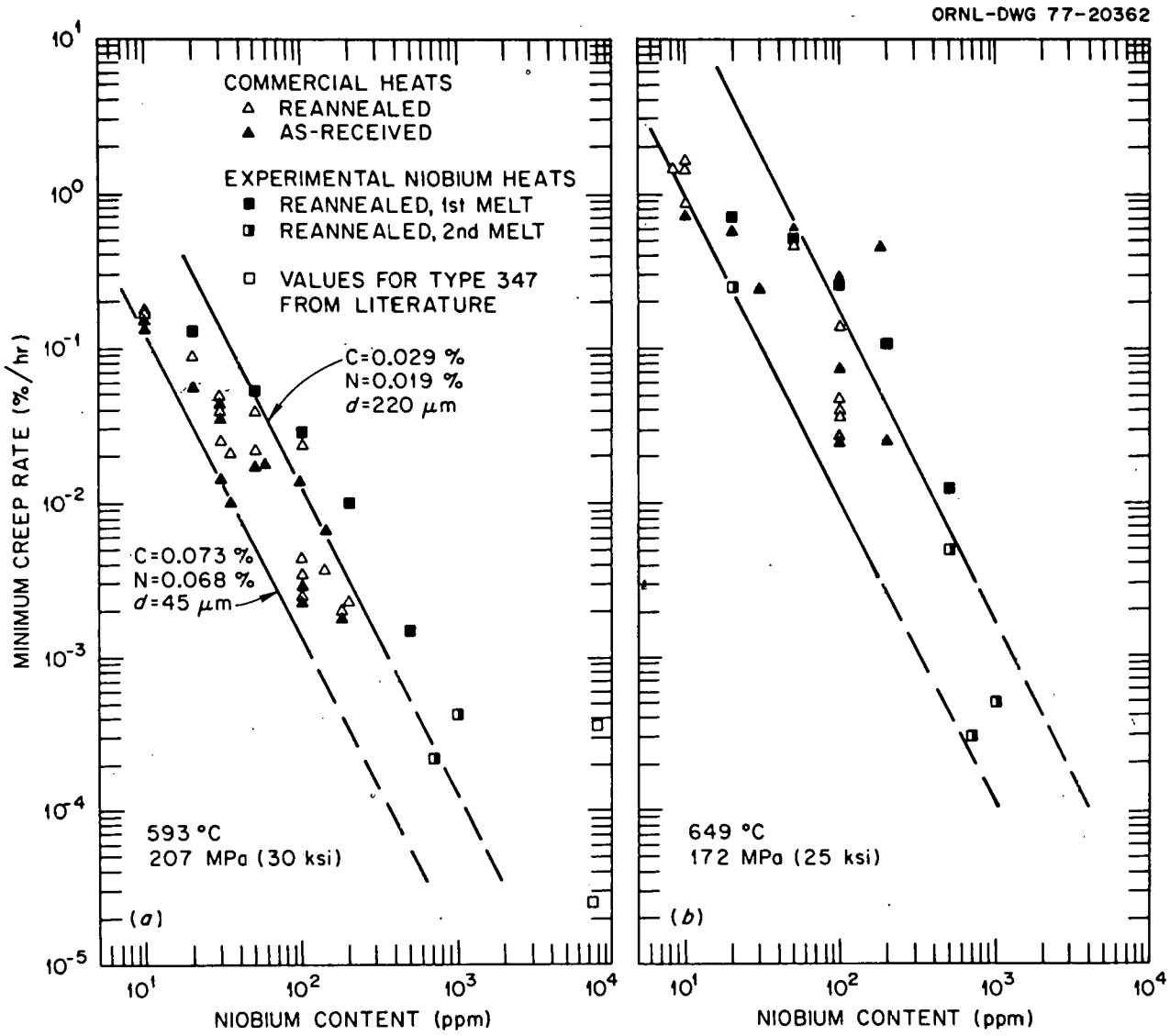

Fig. 6. Minimum Creep Rate as a Function of Nb Content for the Commercial and Experimental Heats of Type 304 Stainless Steel and Commercial Heats of Type 347. (a) at 593°C and 207 MPa, and (b) at 649°C and 172 MPa. Bands in these plots are visual and were drawn to show the trends.

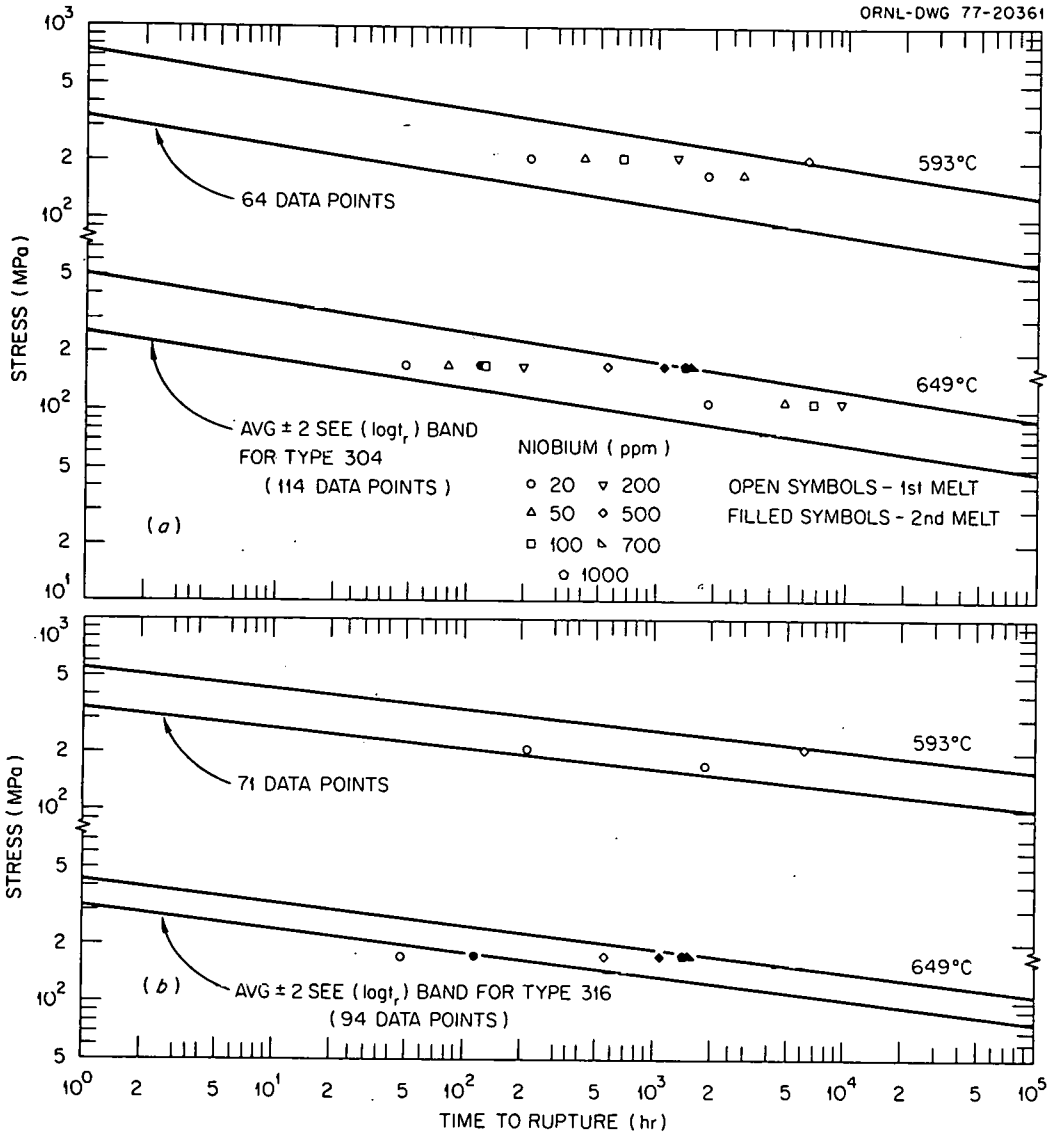

Fig. 7. Comparison of time to rupture data on Nb containing heats with upper and lower data scatter bounds for type 304 and 316 stainless steels at 593 and 649°C. (a) Type 304, (b) type 316.

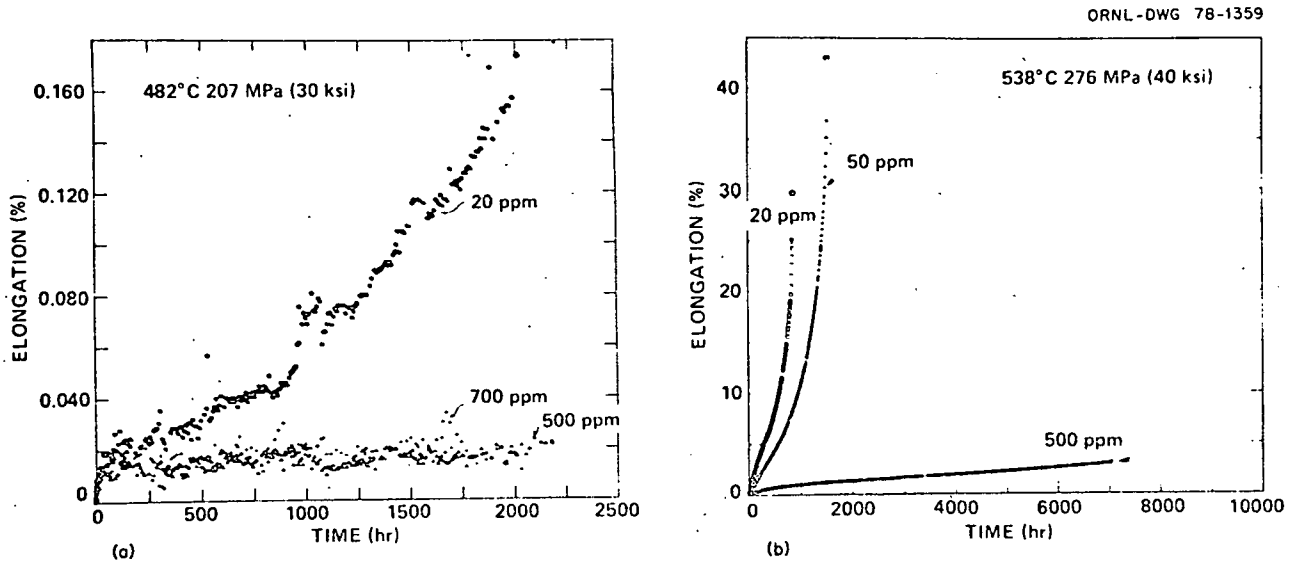

Fig. 8. Creep Curves for Experimental Heats of Type 304 Stainless Steel Containing Various Amounts of Nb. (a) At 482°C and 207 MPa, and (b) at 538°C and 276 MPa. Note the significant improvement in creep resistance for heats containing 500 ppm Nb.

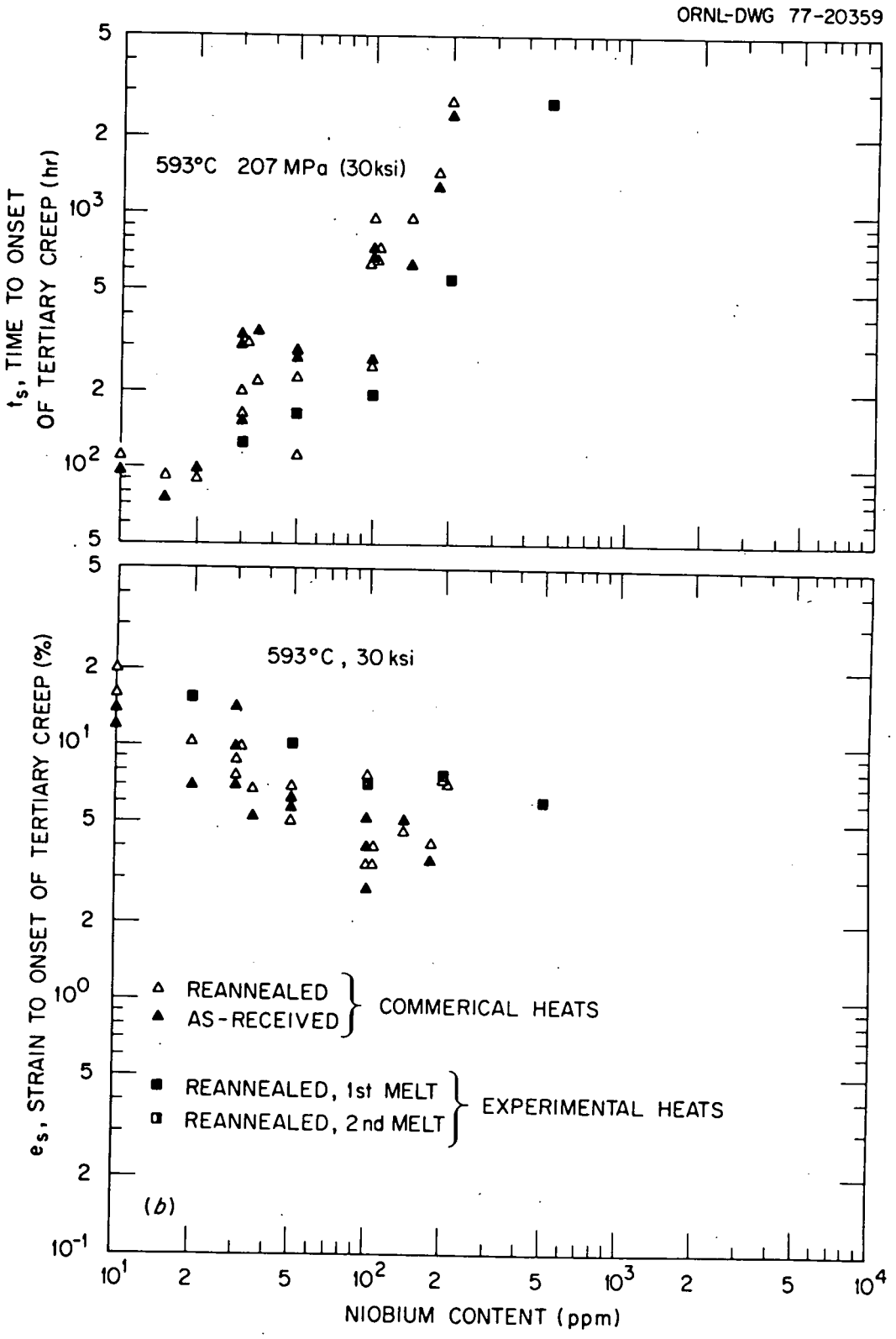

Fig. 9. Tertiary creep data as a function of Nb content for commercial and experimental heats of type 304 stainless steel at 593°C and 207 MPa. (a) Time to onset of tertiary creep, (b) strain to onset of tertiary creep.

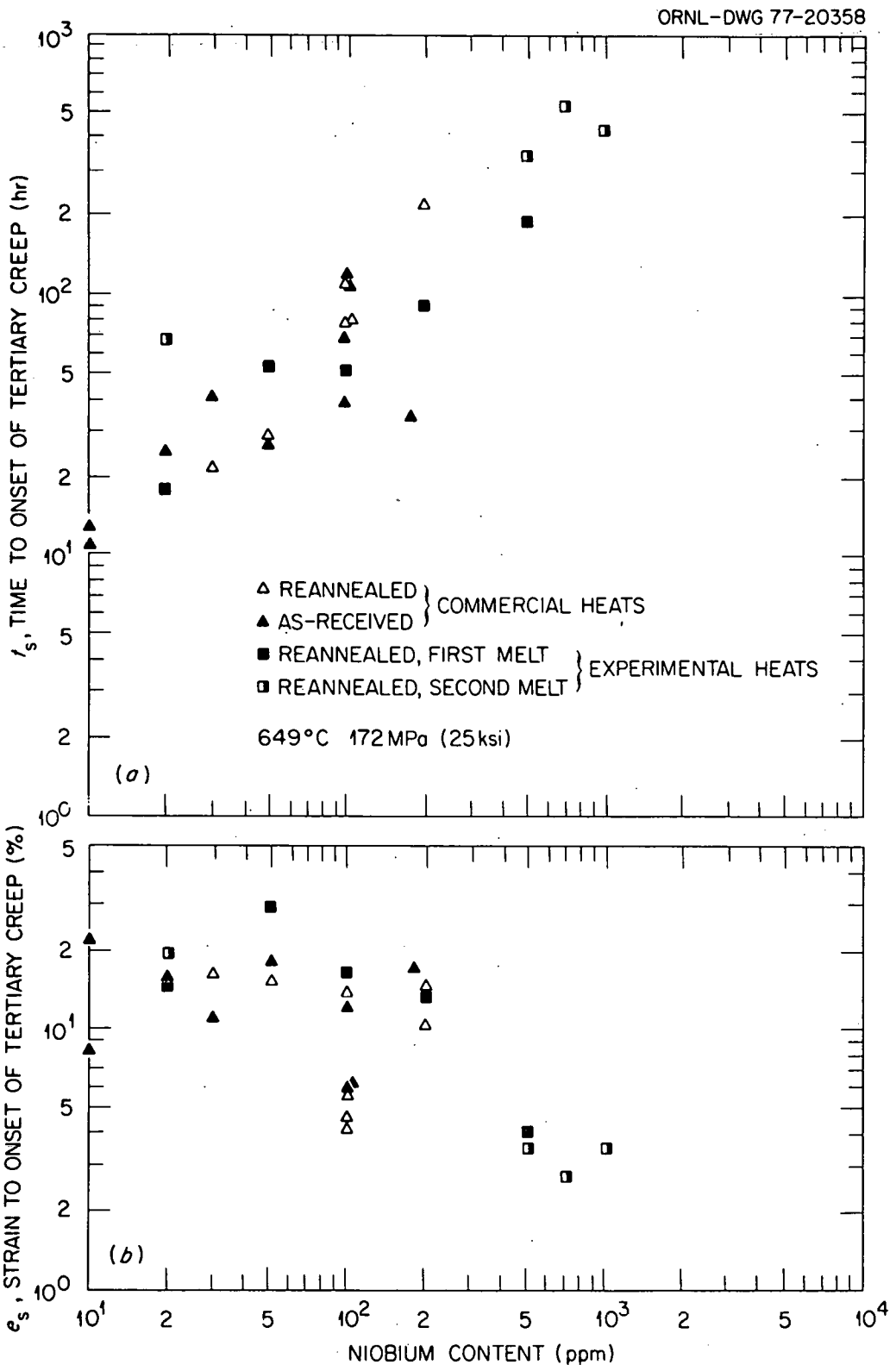

Fig. 10. Tertiary creep data as a function of Nb content for commercial and experimental heats of type 304 stainless steel at 649°C and 172 MPa. (a) Time to onset of tertiary creep, (b) strain to onset of tertiary creep.

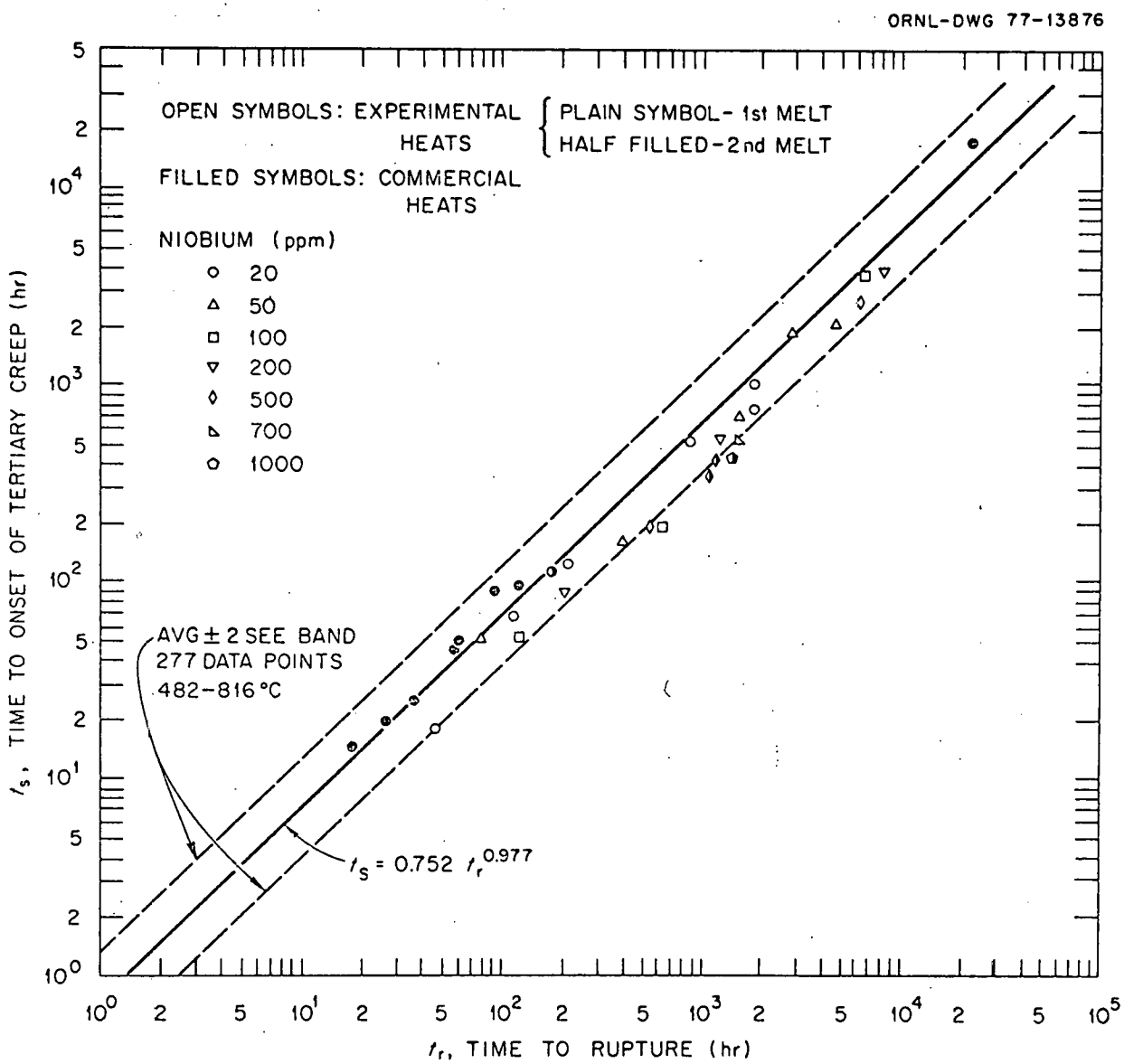

Fig. 11. Comparisons of time to onset of tertiary (t_s) creep data on experimental Nb heats with the average and upper and lower bounds of t_s versus t_r for type 304 stainless steel.

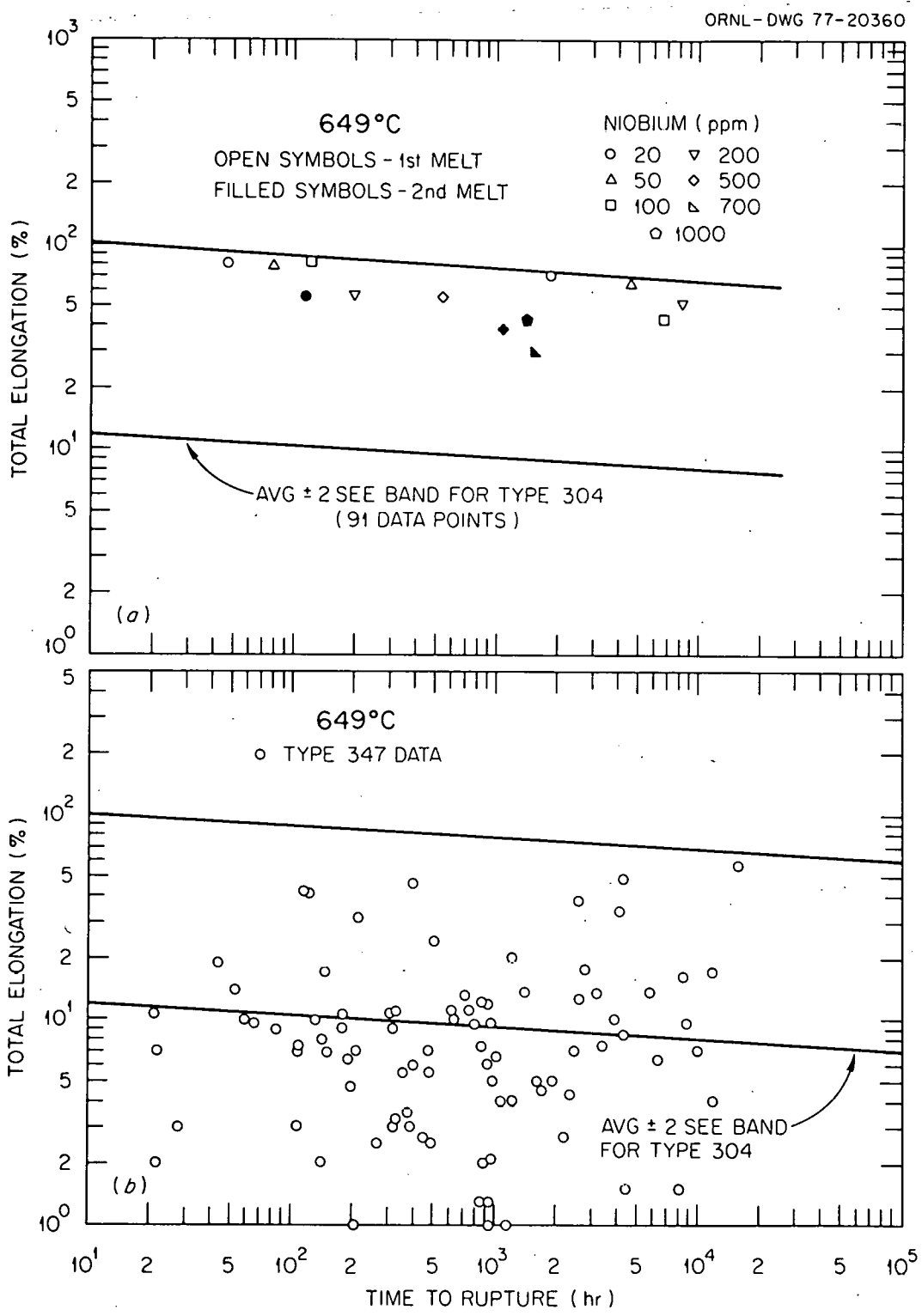

Fig. 12. Comparison of Creep Total Elongation Data on Experimental Nb Heats and Commercial Heats of Type 347 Stainless Steel and Upper and Lower Bounds for Type 304 Stainless Steel. (a) Experimental Nb heats, and (b) type 347.

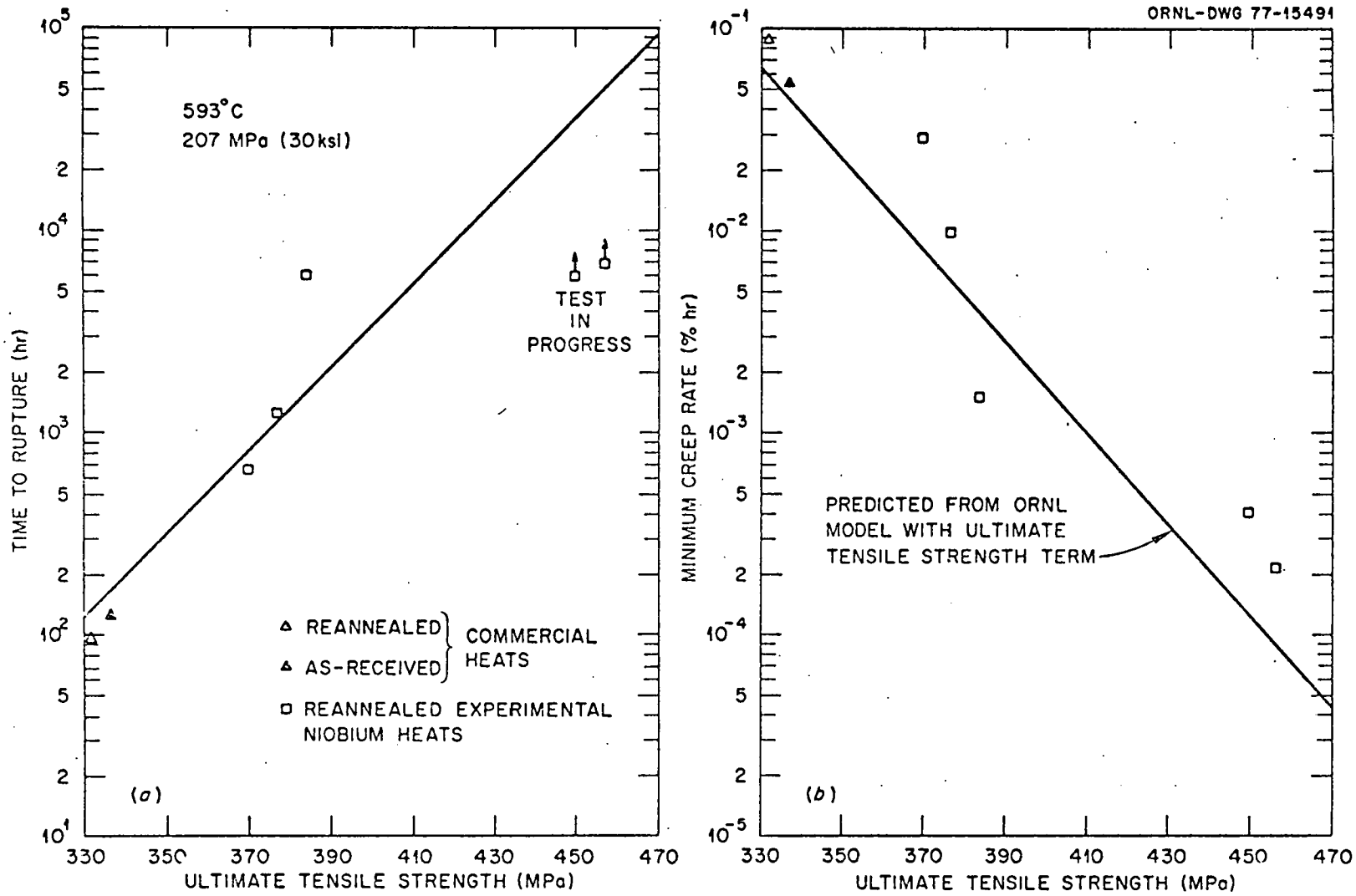

Fig. 13. Plots of creep data on experimental niobium heats at 593°C and 207 MPa as a function of ultimate tensile strength at the creep test temperature. (a) Time to rupture, (b) minimum creep rate. Plots also include predicted curves from ORNL models containing an elevated temperature ultimate tensile strength term.

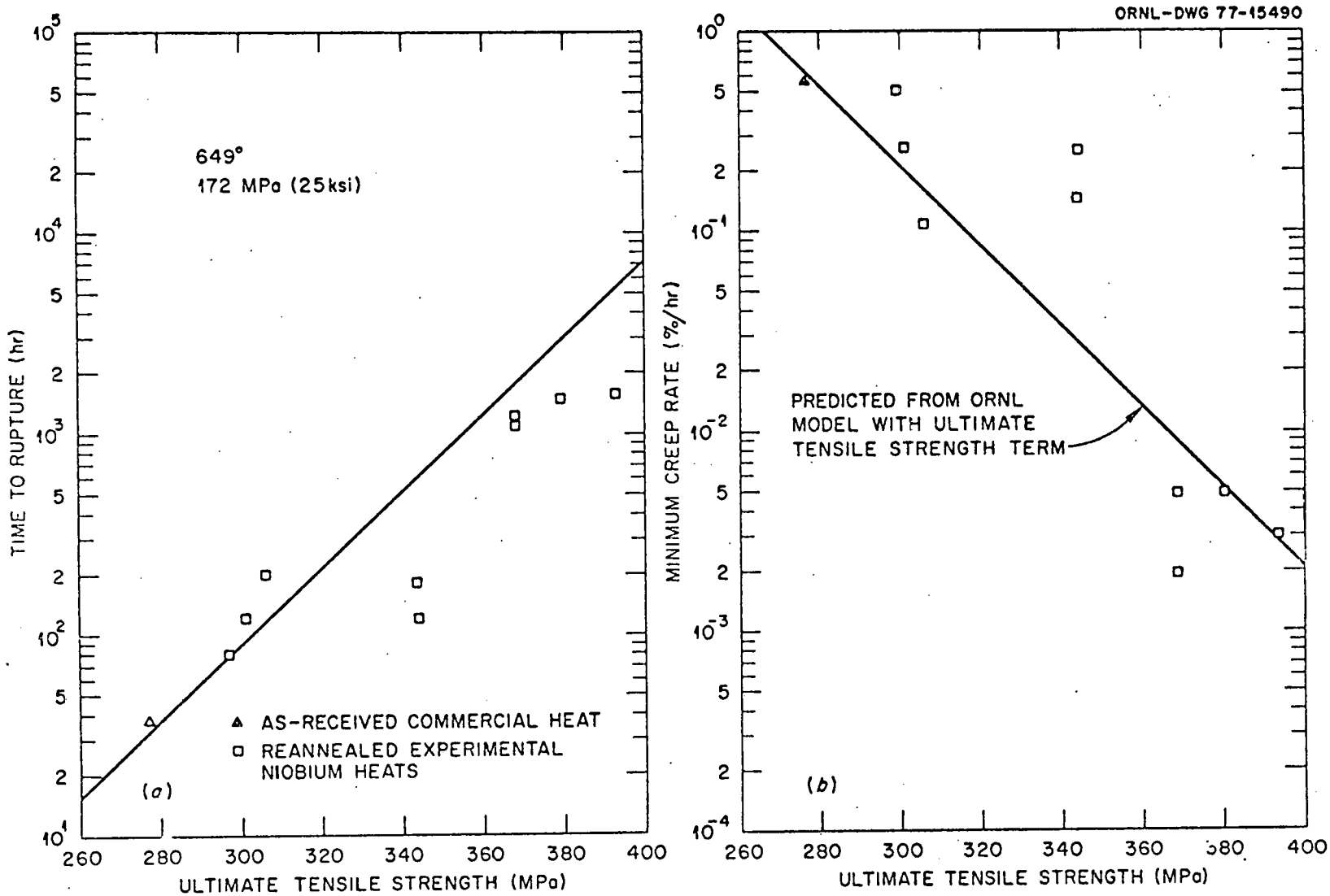

Fig. 14. Plot of creep data on experimental niobium heats at 649°C and 172 MPa as a function of ultimate tensile strength at the creep test temperature. (a) Time to rupture, (b) minimum creep rate. Plots also include predicted curves from ORNL models containing an elevated temperature ultimate tensile strength term.

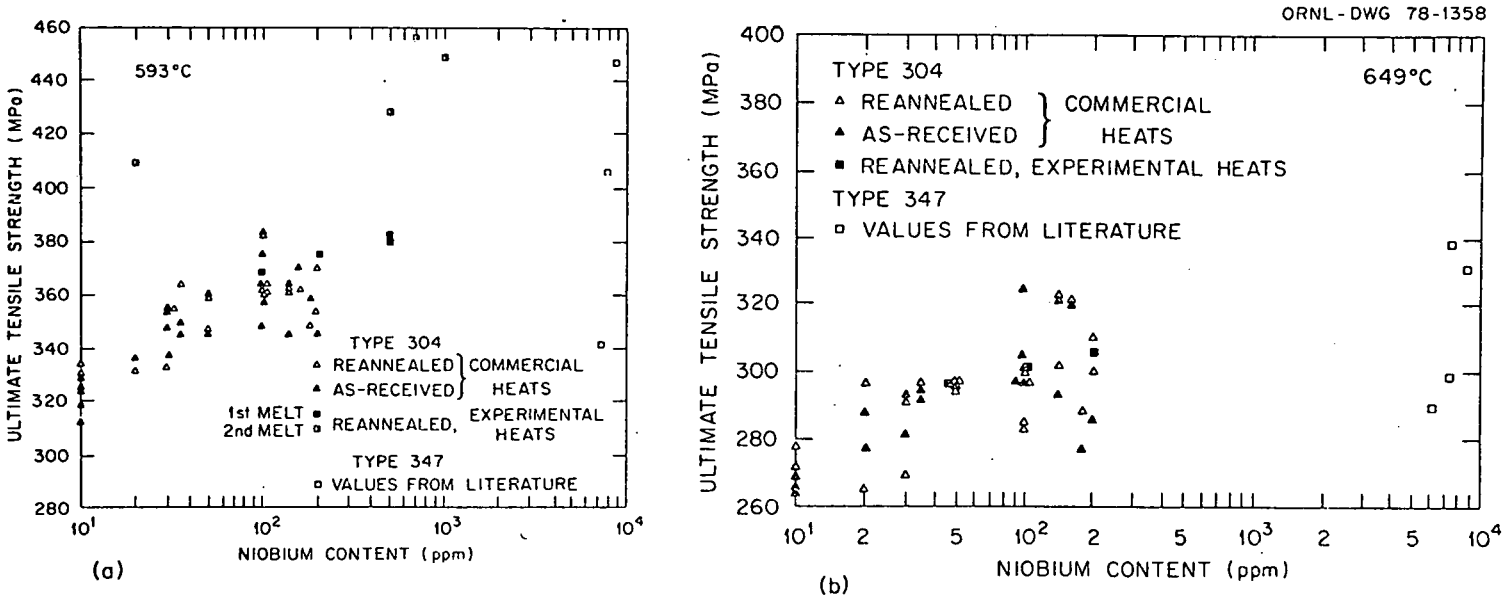

Fig. 15. Plots of ultimate tensile strength as a function of Nb content for commercial and experimental heats of type 304 and commercial heats of type 347 stainless steel. (a) 593°C, (b) 649°C.

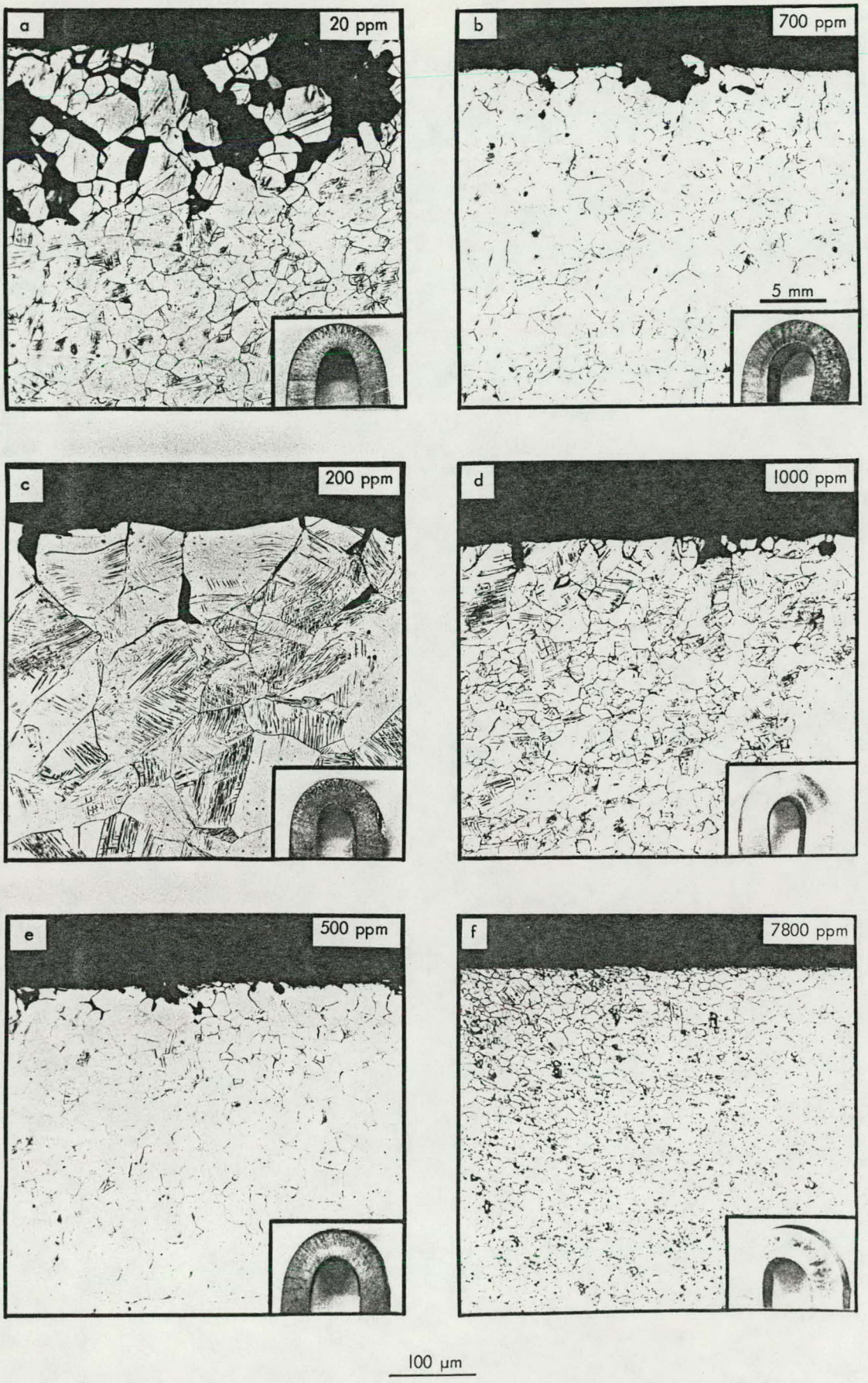

Fig. 16. Micrographs showing improvement in intergranular resistance as a function of increasing Nb (20 to 1000 ppm) in experimental heats of type 304 stainless steel. For comparison, a micrograph on commercial heat of type 347 is also included.

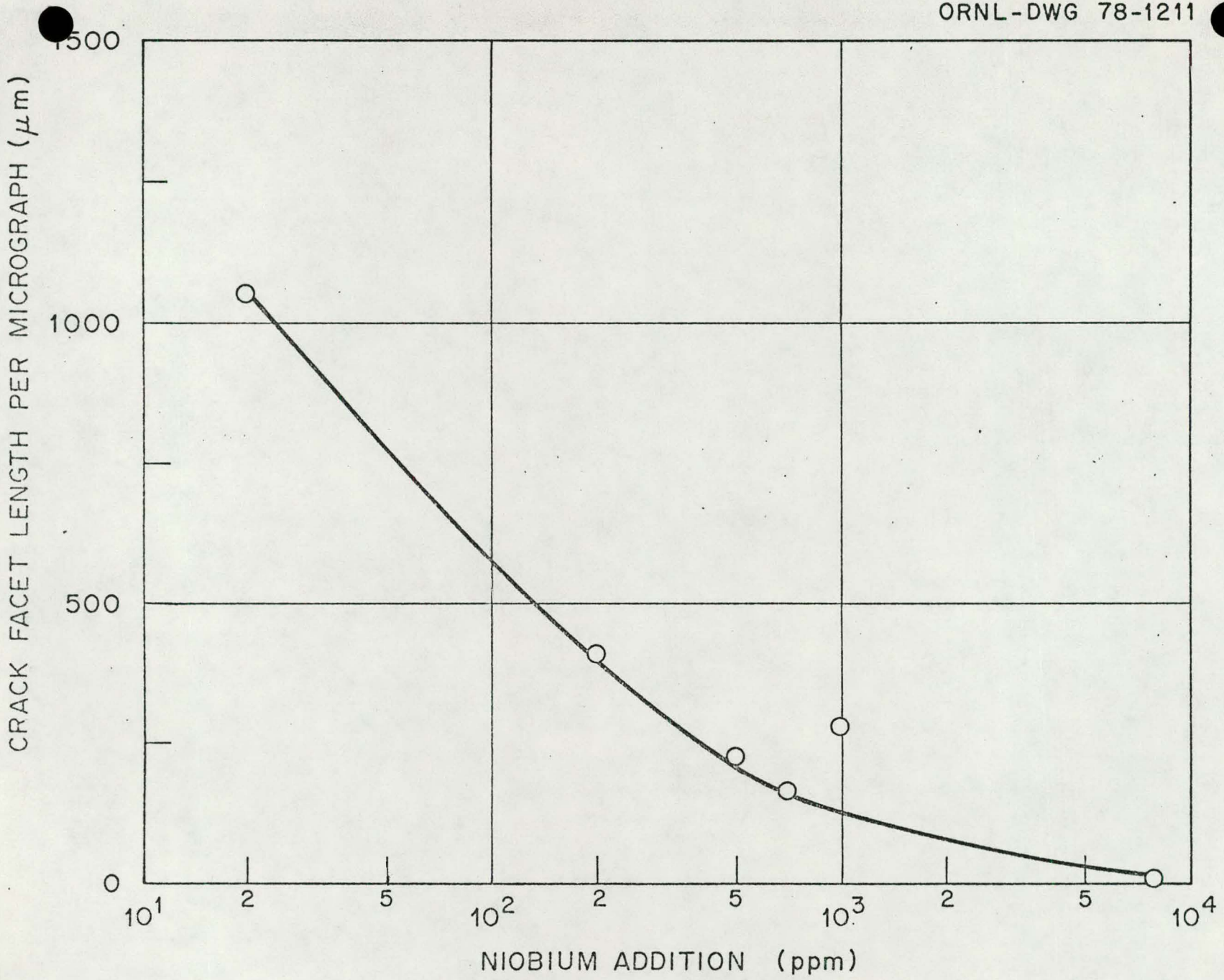

Fig. 17. Plot of Crack Facet Length (CFL) as a Function of Nb Content for Experimental Heats of Type 304 Stianless Steel and a Commercial Heat of Type 347. The CFL values in this plot are from same size micrographs on each heat.

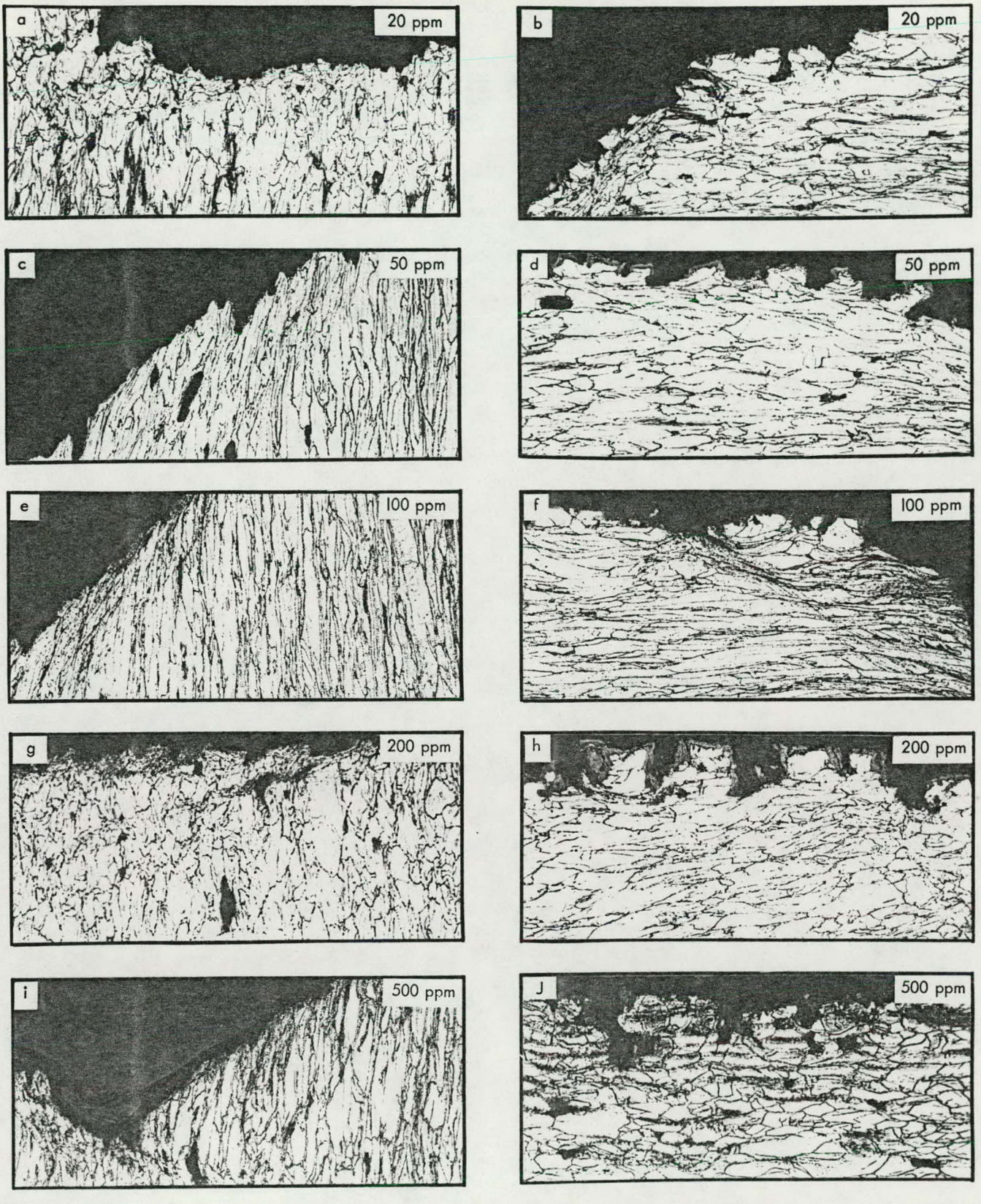

Fig. 18. Micrographs showing fracture and edge near the fracture for specimens creep tested at 649°C and 172 MPa. (a) and (b) 20 ppm, (c) and (d) 50 ppm, (e) and (f) 200 ppm, (g) and (h) 500 ppm. All specimens were annealed at 1065°C for 0.5 hr prior to creep testing. Note that there are no significant differences between the fracture of specimens containing various niobium content.

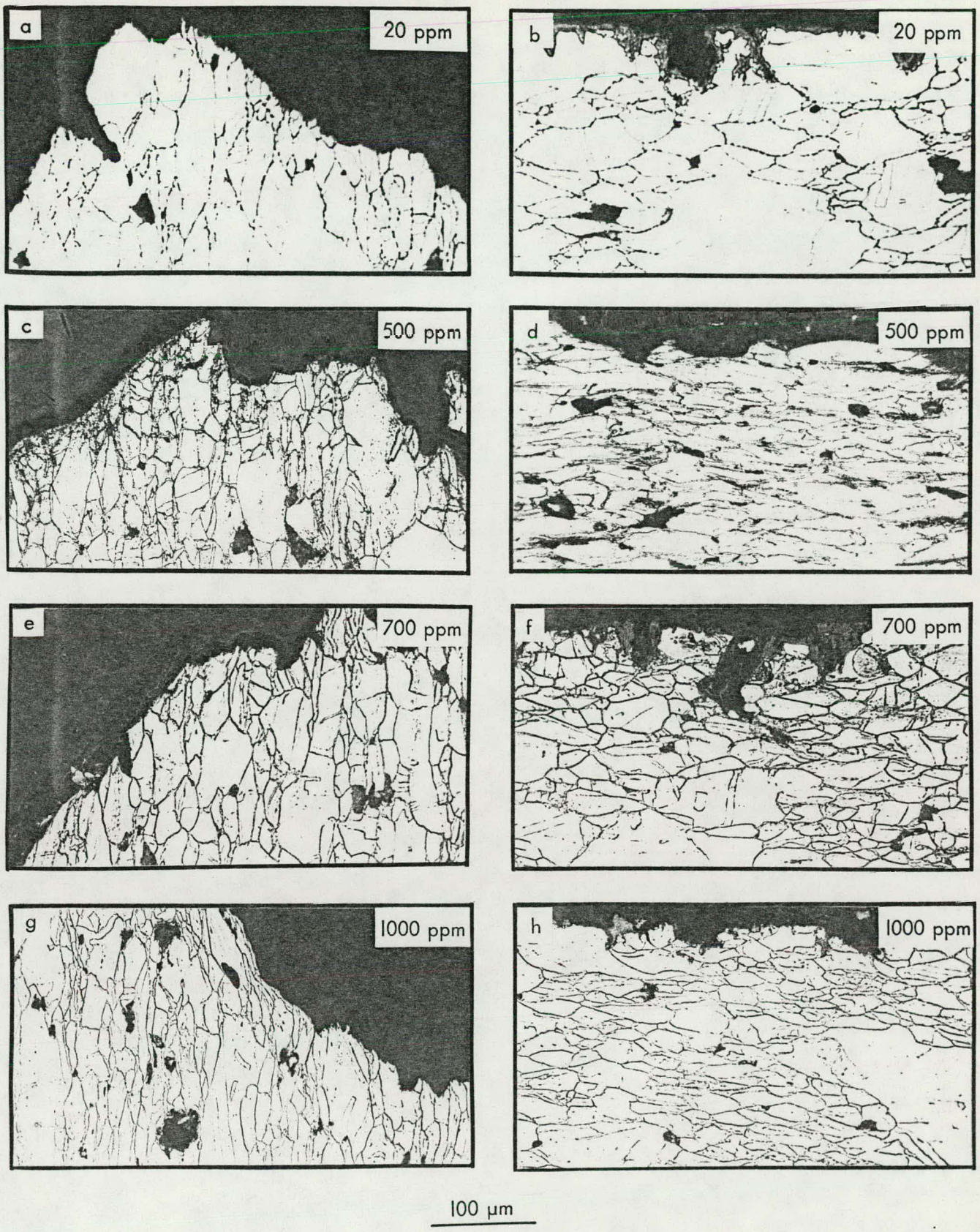

Fig. 19. Micrographs showing fracture and edge near the fracture for specimens creep tested at 649°C and 172 MPa. (a) and (b) 20 ppm, (c) and (d) 500 ppm, (e) and (f) 700 ppm, and (g) and (h) 1000 ppm. All specimens were from second melt and were annealed at 1065°C for 0.5 hr prior to creep testing. Note that there are no obvious microstructural differences between the first and second melt.

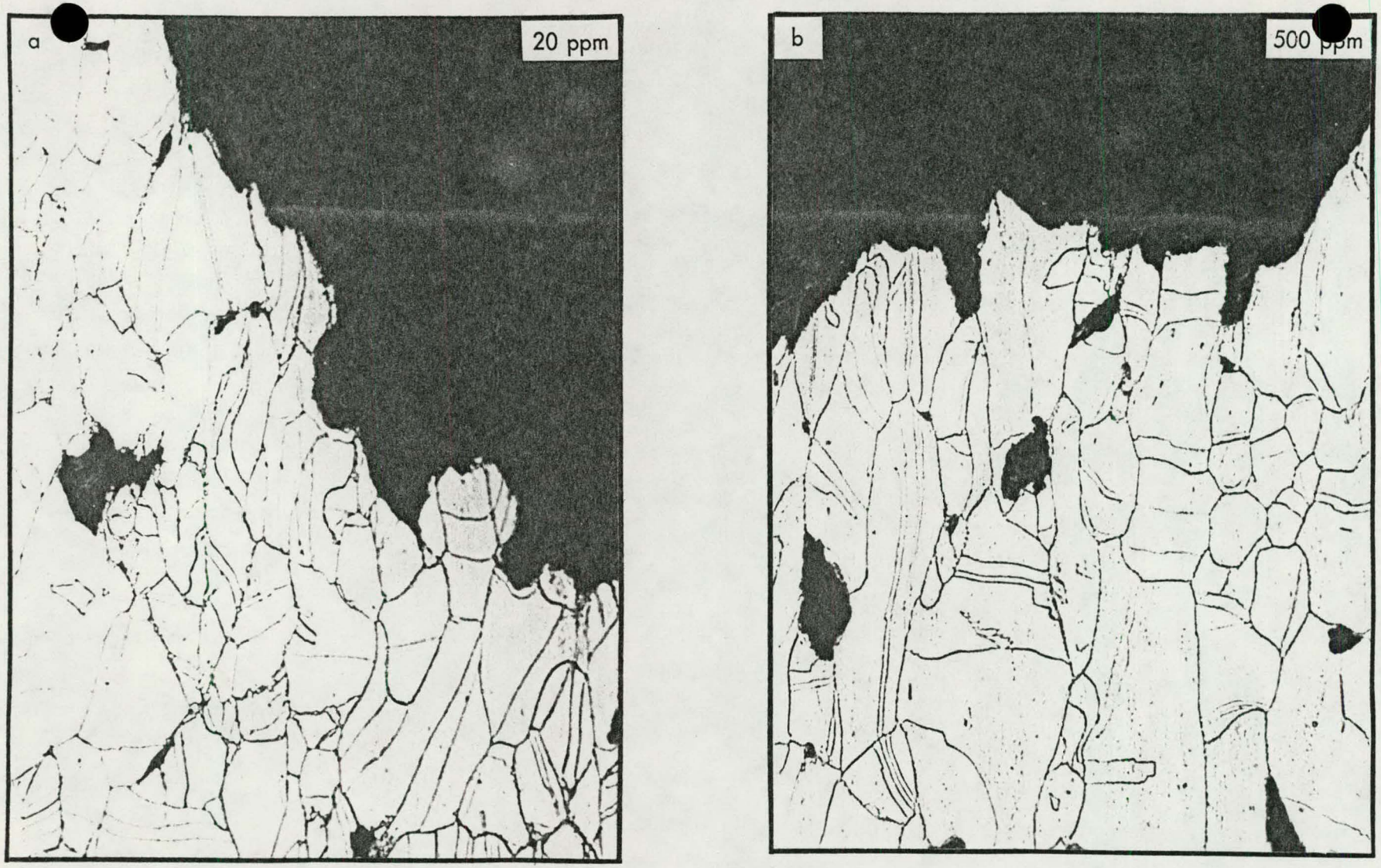

Fig. 20. Micrographs showing fracture for specimens annealed at 1150°C for 0.5 hr and creep tested at 649°C and 172 MPa. (a) 20 ppm (b) 500 ppm. The 1150°C annealed specimens had slightly coarser grain size than observed in Fig. 18 and 19 for the 1065°C annealed specimens.

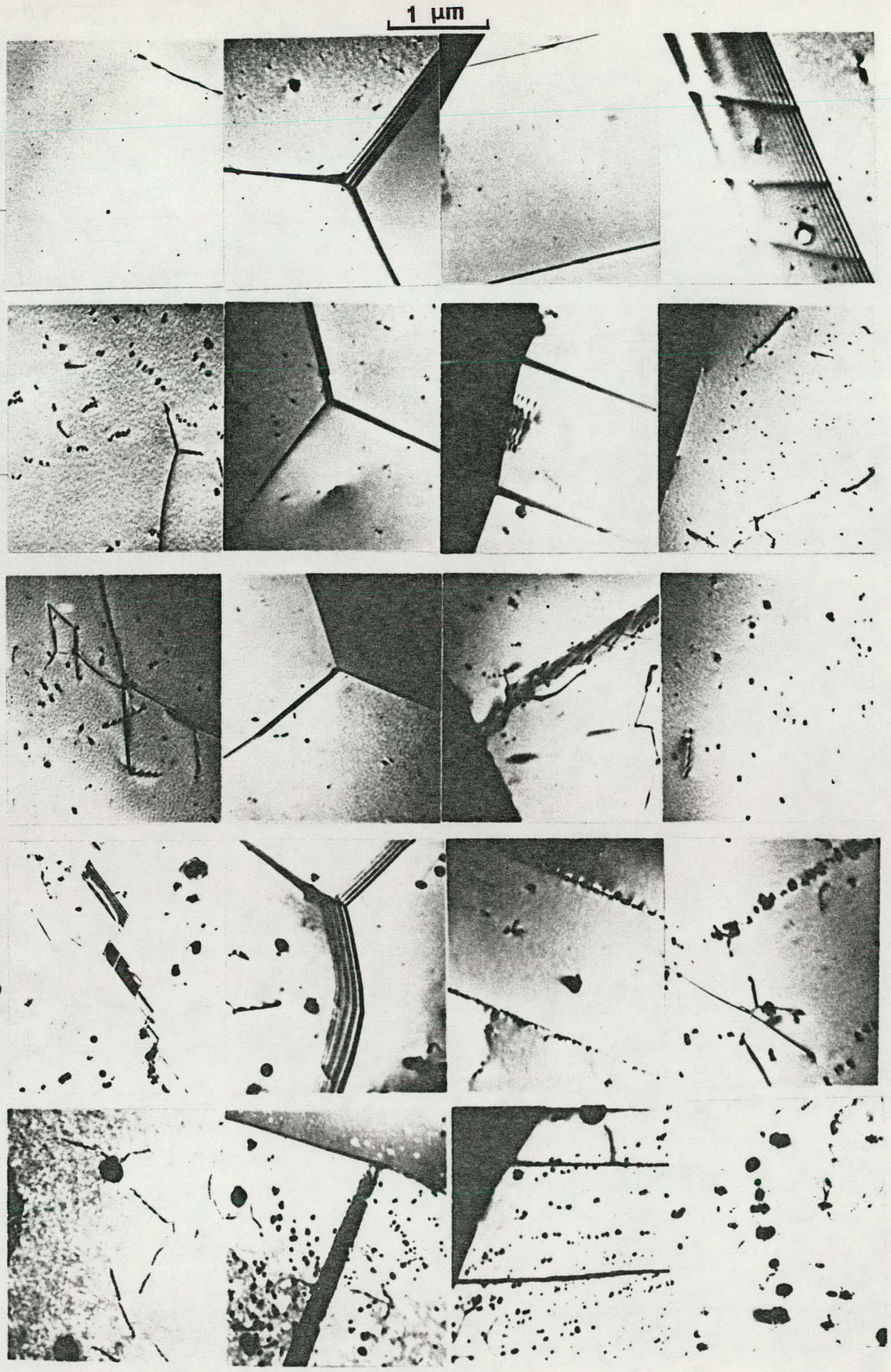

Fig. 21. Transmission electron micrographs for experimental heats of type 304 containing varying amounts of Nb and on a commercial heat of reannealed type 347 stainless steel. Note the difference in precipitation with increasing Nb content.

Table 1. Summary of Vendor, Product Form, and Grain Size of 20 Heats of Type 304 Stainless Steel

Heat	Heat Symbol	Vendor	As Received Form	Dimension		Grain Size[a]			
						As Received		Reannealed	
				(mm)	(in.)	(ASTM)	(μm)	(ASTM)	(μm)
9T2796	796	USS	Plate	50.8	2.00	0.26	280	0.26	280
X22807	807	USS	Plate	63.5	2.50	4.7	61	4.6	64
9T2797	797	USS	Plate	25.4	1.00	3.2	103	2.2	150
R23283	283	USS	Plate	19.0	0.75	5.2	52	4.8	60
R22926	926	USS	Plate	50.8	2.00	3.6	90	3.5	94
337187	187	Allegheny Ludlum	Plate	38.1	1.50	2.1	150	2.3	140
55697	697	Allegheny Ludlum	Bar	15.9	0.63	2.9	115	1.0	220
345866	866	Allegheny Ludlum	Plate	76.2	3.00	4.2	73	3.2	103
346544	544	Allegheny Ludlum	Plate	50.8	2.00	4.0	78	5.4	48
337330	330	Allegheny Ludlum	Plate	28.6	1.13	5.6	45	5.0	55
346845	845	Allegheny Ludlum	Plate	69.9	2.75	3.8	84	4.0	78
346779	779	Allegheny Ludlum	Plate	63.5	2.50	4.1	76	4.4	68
310390	390	Carlson	Plate	50.8	2.00	3.4	97	3.4	97
600414	414	Carlson	Plate	60.3	2.38	3.7	97	2.7	140
60551	551	Carlson	Bar	127 x 178	5 x 7	4.0	78	3.7	87
616737	737	Carlson	Plate	66.7	2.63	4.0	78	3.2	104
300380	380	Carlson	Plate	60.3	2.38	4.0	78	4.6	64
544086	086	Carlson	Plate	25.4	1.00	5.8	42	4.6	64
8043813	813	Republic	Plate	25.4	1.00	3.8	84	4.0	78
3121	121	Cameron	Pipe	710 x 9.5	28 OD x $\frac{3}{8}$ wall	1.1	215	1.7	175

[a]Method of J. E. Hillard, "Estimating Grain Size by the Intercept Method," *Met Prog.* 85(5): 98–102 (May 1964).

Table 2. Summary of Chemical Analysis of 20 Heats of Type 304 Stainless Steel

Heat Symbol	Content, %																				
	C	N	P	B	O	H	Ni	Mn	Cr	Si	Mo	S	Nb	V	Ti	Ta	W	Cu	Co	Pb	Sn
796	0.047	0.031	0.029		0.0110	0.0006	9.58	1.22	18.5	0.47	0.10	0.012	0.008	0.037	0.003	<0.0005	0.022	0.10	0.05	0.01	0.02
807	0.029	0.021	0.024	0.0005	0.010	0.0012	9.67	1.26	18.8	0.50	0.20	0.023	0.0015	0.012	0.002	<0.0005	0.020	0.11	0.03	0.01	0.01
797	0.059	0.055	0.028	0.0020	0.0075	0.0007	9.78	1.49	18.3	0.60	0.30	0.011	0.0050	0.020	0.005	0.0005	0.050	0.30	0.07	0.002	0.005
283	0.043	0.025	0.018	0.0003	0.0140	0.0009	9.12	1.32	18.2	0.45	0.30	0.020	0.0030	0.030	0.0010	<0.0005	0.021	0.14	0.05	0.01	0.01
926	0.053	0.041	0.020		0.0084	0.0007	9.79	1.16	19.0	0.68	0.10	0.025	0.0180	0.050	0.0100	0.0010	0.030	0.070	0.05	0.010	0.02
187	0.068	0.031	0.018		0.0042	0.0005	9.43	0.83	18.2	0.59	0.07	0.008	0.0020	0.060	0.003	<0.0005	0.015	0.15	0.05	0.01	0.02
697	0.057	0.034	0.016		0.0150	0.0005	9.38	0.91	18.5	0.50	0.05	0.037	0.0030	0.030	0.002	<0.0005	0.011	0.10	0.05	0.01	0.02
866	0.044	0.022	0.023	0.0002	0.0096	0.0010	8.98	1.51	18.5	0.47	0.2	0.007	0.0010	0.018	0.0005	0.0005	0.007	0.13	0.04	0.01	0.01
544	0.063	0.019	0.023	0.0002	0.0081	0.0006	9.12	0.99	18.4	0.47	0.2	0.006	0.0050	0.025	0.017	0.0006	0.026	0.12	0.05	0.01	0.01
330	0.068	0.031	0.018		0.0042	0.0005	9.43	0.83	18.2	0.59	0.07	0.008	0.0100	0.025	0.002	<0.0005	0.0060	0.15	0.05	0.01	0.02
845	0.057	0.024	0.023	0.0002	0.0092	0.0013	9.28	0.92	18.4	0.53	0.10	0.006	0.0100	0.050	0.008	<0.0005	0.007	0.11	0.07	0.01	0.01
779	0.065	0.023	0.024	0.0002	0.0056	0.0009	9.46	0.94	18.1	0.47	0.20	0.005	0.0035	0.029	0.010	0.0020	0.043	0.16	0.02	0.01	0.01
390	0.066	0.086	0.018	0.0020	0.0052	<0.0001	8.75	1.57	18.6	0.60	0.30	0.006	0.0160	0.020	0.001	0.0006	0.043	0.20	0.07	0.0007	0.002
414	0.073	0.058	0.016		0.0190	0.0004	9.52	0.94	18.7	0.69	0.10	0.015	0.0100	0.025	0.002	<0.0005	0.027	0.10	0.05	0.01	0.02
551	0.043	0.027	0.022	0.0010	0.0220	0.0013	9.40	1.20	18.5	0.59	0.30	0.018	0.0140	0.050	0.025	<0.0005	0.049	0.25	0.08	0.01	0.01
737	0.064	0.075	0.026	0.00005	0.0072	<0.0001	9.01	1.71	18.3	0.50	0.30	0.012	0.0140	0.031	0.001	<0.0005	0.016	0.50	0.07	<0.0003	0.0050
380	0.063	0.068	0.018		0.0260	0.0009	8.30	0.97	18.4	0.55	0.07	0.010	0.0100	0.028	0.004	<0.0005	0.016	0.10	0.05	0.01	0.02
086	0.050	0.043	0.025		0.0091	0.0005	9.46	1.23	18.4	0.53	0.20	0.016	0.0030	0.019	0.006	<0.0005	0.021	0.10	0.05	0.01	0.02
813	0.062	0.033	0.044	0.0003			8.95	1.87	17.8	0.48	0.32	0.004	0.0200	0.022	0.002	<0.0005	0.02				
121	0.065	0.140	0.019	0.00005	0.0026	0.0011	9.19	1.92	18.1	0.30	0.14	0.010	0.0010	0.035	0.016	<0.0005	0.015	0.07	0.07	<0.0003	0.002

Table 3. Summary of chemical analysis and grain size of type 304 stainless steel containing small niobium additions. Table also contains chemical analysis of a type 347 plate used for corrosion studies.

Heat No.	187[a,b]	187-1[c,b]	187-1-A[d,e]	187-2[c,b]	187-3[c,b]	187-4[c,b]	187-5[c,b]	187-5-A[d,e]	187-6-A[d,e]	187-7-A[d,e]	Type 347[e]
Grain size (intercept) ASTM (μm)	2.3 (140)	6 (38)	7.7 (22)	6 (38)	6 (38)	6.2 (36)	6.6 (33)	7.9 (21)	7.8 (21)	7.9 (20)	<9 (~10)
Chemical composition											
Carbon	0.068	0.0488	0.052	0.0484	0.0485	0.0575	0.0480	0.049	0.050	0.051	0.070
Nitrogen	0.031	0.028	0.029	0.0270	0.0270	0.0290	0.0290	0.030	0.028	0.029	0.039
Phosphorus	0.018	0.023	0.029	0.0220	0.0190	0.020	0.0230	0.028	0.029	0.029	0.040
Boron		0.0002	0.0010	0.0002	0.0002	0.0002	0.0002	0.001	0.001	0.001	0.001
Oxygen	0.0042	0.0020		0.0028	0.0051	0.0035	0.0029				
Hydrogen	0.0005	0.0004		0.0002	0.0008	0.0004	0.0006				
Nickel	9.43	9.63	9.48	9.32	9.62	9.92	9.75	9.53	9.57	9.51	11.50
Manganese	0.83	0.99	0.96	0.96	0.98	0.91	0.96	0.94	0.96	0.95	1.53
Chromium	18.20	18.30	18.22	17.6	18.40	18.40	18.20	18.13	18.18	18.10	17.05
Silicon	0.59	0.46	0.44	0.50	0.60	0.57	0.56	0.43	0.44	0.43	0.68
Molybdenum	0.07	0.15	0.14	0.21	0.25	0.24	0.24	0.14	0.15	0.14	0.41
Sulfur	0.008	0.0055	0.009	0.0055	0.0050	0.0050	0.0055	0.009	0.009	0.009	0.006
Niobium	0.0020	0.0020	<0.01	0.0050	0.010	0.020	0.05	0.05	0.07	0.10	0.78
Vanadium	0.060		0.06					0.06	0.06	0.06	0.03
Titanium	0.003	0.01	<0.01	0.01	0.01	0.01	0.01	<0.01	<0.01	<0.01	<0.01
Tantalum	<0.0005	0.001		0.001	0.001	<0.001	<0.001				
Tungsten	0.015	0.05		0.05	0.05	0.05	0.05				
Copper	0.15	0.10	0.12	0.1	0.1	0.1	0.1	0.12	0.12	0.12	0.20
Cobalt	0.05	0.10	0.10	0.1	0.1	0.1	0.1	0.10	0.10	0.10	0.12
Lead	0.01	<0.001		<0.001	<0.001	<0.001	<0.001				
Tin	0.02	0.005		0.005	0.005	0.005	0.005				
Aluminum		0.005	0.01	0.005	0.005	0.01	0.005	<0.01	<0.01	<0.01	<0.01

[a] Commercial type 304.

[b] Analysis performed at ORNL.

[c] First melt.

[d] Second melt.

[e] Analysis performed at Combustion Engineering.

Table 4. Summary of Creep Data on Type 304 Stainless Steel Containing Small Niobium Additions

Test #	Specimen Number	Condition[a]	Temperature (°C)	Stress (MPa)	Strain, %						Time, hr				Minimum Creep Rate $\dot{e}_m$ (%/hr)	RA (%)
					Loading e_l	Transient e_{pc}	Primary e_1	Secondary e_2	0.2% Offset e_3	Fracture e_f	Primary t_1	Secondary t_2	0.2% Offset t_s	Rupture t_r		
								20 ppm Nb Commercial								
9680	187 15	A240	538	317	16.61	0.05	0.10	5.40	5.90	30.21	8.5	47.0	49.5	60.7	0.113	27.53
9443	187 4	A240	593	117	0.47	1.00	1.25	2.55	2.93	9.97	3000.0	15,500.0	17,500.0	22622.2	9625E-5	8.80
9375	187 3	A240	593	207	4.34	1.25	2.80	6.05	6.90	13.44	28.0	85.0	98.0	120.5	0.0525	6.33
9471	187 6	1065	593	207	6.71	2.00	4.63	9.63	10.31	27.71	29.5	87.0	91.0	92.7	0.088	21.35
9475	187 5	1065	593	241	7.05	0.40	1.00	5.50	6.30	22.85	2.0	17.3	19.3	25.8	0.290	22.65
9369	187 2	A240	593	241	6.01	0.50	1.30	4.70	5.70	23.71	2.3	12.5	14.8	18.3	0.335	20.45
14500	187 21	1065	593	241	9.96	1.70	3.78	9.15	10.48	27.28	11.5	40.8	46.7	59.2	0.183	25.22
9669	187 14	A240	649	172	4.00	1.00	2.45	10.25	15.25	35.60	2.8	20.5	25.0	36.8	0.560	31.20
								20 ppm Experimental								
18118	1871 C2	1065	482[b]	207	2.98									2008.4		2.86
17316	1871 3	1065	538	276	10.09	0.75	2.25	7.25	8.25	39.71	125.0	450.0	515.0	863.0	0.0147	48.86
17347	1871 6	1065	593	172	2.82	1.15	2.10	15.00	15.50	65.20	52.0	745.0	770.0	1859.0	0.0184	70.65
16683	1871 1	1065	593	207	5.68	1.50	3.50	13.50	15.50	63.36	17.5	97.5	111.3	215.5	0.128	63.13
17177	1871 5	1093	649	110	0.69	2.75	8.50	17.50	18.75	69.71	360.0	925.0	1000.0	1871.71	0.0156	64.09
16880	1871 2	1065	649	110	0.74	2.25								1061.3	0.0199	18.78
17339	1871 4	1065	649	172	3.31	2.00	3.50	14.00	15.00	80.67	2.5	16.5	18.0	47.1	0.7100	78.10
17913	1871 C1	1065	649	172	2.34	1.50	3.50	16.00	19.50	56.47	8.0	57.0	69.0	116.5	0.2520	54.50
18535	1871 C6	1150	649	172	2.61	2.25	6.00	16.75	18.75	47.27	26.0	101.0	113.0	176.9	0.1425	44.47
								50 ppm Experimental								
17392	1872 5	1065	538	276	9.46	0.13	1.25	5.00	6.50	52.39	130.0	570.0	700.0	1531.0	0.0087	58.20
17502	1872 4	1065	593	172	2.79	3.00	8.75	24.00	26.00	72.10	500.0	1775.0	1900.0	2835.5	0.0126	73.75
16700	1872 1	1065	593	207	5.23	1.50	4.00	9.00	10.25	64.09	50.0	142.5	162.5	409.9	0.0530	70.48
16873	1872 2	1065	649	110	0.80	4.00	6.50	10.00	11.25	63.88	675.0	1750.0	2075.0	4692.6	0.0033	61.99
17337	1872 3	1065	649	172	3.03	2.00	3.50	28.50	29.50	79.50	3.5	52.0	53.6	79.0	0.5100	79.27
								100 ppm Experimental								
16694	1873 1	1065	593	207	4.37	1.50	2.75	6.00	7.25	54.70	45.0	150.0	190.0	654.2	0.0290	72.63
16874	1873 2	1064	649	110	0.90	3.88	5.00	8.75	9.75	42.97	800.0	3200.0	3700.0	6646.9	0.0017	61.25
17340	1874 3	1065	649	172	2.58	2.50	5.00	15.00	16.50	82.48	8.0	47.5	53.0	121.9	0.2600	81.58
								200 ppm Experimental								
16697	1874 1	1065	593	207	5.49	1.75	3.00	6.25	7.50	47.26	120.0	450.0	550.0	1249.6	0.0099	62.86
17129	1874 2	1065	649	110	0.55	2.00	2.25	4.25	5.00	51.16	475.0	3500.0	3900.0	8295.1	6.5E-4	57.35
17344	1874 3	1065	649	172	2.78	3.00	5.00	11.50	13.00	56.40	18.0	80.0	92.0	199.0	0.1075	71.74
								500 ppm Experimental								
18123	1875 C2	1065	482[b]	207	2.63									2183.6		2.62
17697	1875 5	1065	538	276	7.86	0.625	0.875	2.25	3.250	30.05	900.0	5500.0	7800.0	14,585.0	2.9E-4	41.49
16701	1875 1	1065	593	207	4.00	1.50	1.75	5.00	6.00	30.62	150.0	2350.0	2750.0	6121.9	1.5E-3	47.61
17527	1875 2	1065	649	110	0.64	1.00	1.25	2.50	3.00	45.10	500.0	3600.0	4300.0	11404.2	3.75E-4	62.41
17911	1875 C1	1065	649	172	1.78	1.50	2.00	3.00	3.50	38.27	90.0	290.0	350.0	1097.3	0.0048	35.04
18567	1875 C6	1150	649	172	2.31	0.75	0.88	1.25	1.75	37.19	40.0	300.0	430.0	1186.7	0.0019	46.91
17346	1875 3	1065	649	172	2.92	1.45	2.05	3.10	4.05	55.21	50.0	135.0	195.0	545.0	0.0121	72.41
								700 ppm Experimental								
18246	1876 B3	1065	482	207	2.41									2033.0		2.91
17912	1876 B1	1065	593[c]	207	2.55	0.54								14,373.0	2.2E-4	
17941	1876 B2	1065	649	172	1.80	0.88	1.00	2.00	2.75	29.08	50.0	400.0	550.0	1592.1	0.0029	43.45
								1000 ppm Experimental								
17956	1877 B1	1065	593	207	2.69	1.08								13,627.0	4.3E-4	
17958	1877 B2	1065	649	172	1.90	1.25	1.75	2.75	3.50	43.29	120.0	330.0	440.0	1433.9	0.0048	56.76
18710	1877 B6	1150	649	172	2.03	0.375	0.425	0.75	1.125	41.46	12.5	525.0	800.0	2695.4	0.00065	53.86

[a] A240 = as-received, 1065, 1093, and 1150°C indicate annealing temperatures for 0.5 hr durations

[b] Tests discontinued prior to rupture

[c] Tests in progress

Table 5. Summary of Tensile Data on Type 304 Stainless Steel Containing Small Niobium Additions.

Test No.	Specimen No.	Condition	Temp. °C	Proportional limit	Stress, Mpa (ksi) Yield 0.02%	Yield 0.2%	Ultimate	Elongation Uniform	Elongation Total 25.4 mm	RA %
					20 ppm Experimental					
18248	1871 C3	1065	593	57 (8.2)	87 (12.6)	109 (15.8)	409 (59.3)	28.18	37.70	70.14
18713	1871 C4	1065/1250	593	55 (7.9)	72 (10.4)	81 (11.7)	434 (63.0)	29.93	37.85	59.27
18984	1871 C5	1093	649	42 (6.1)	66 (9.6)	98 (14.2)	344 (49.9)	28.51	52.60	65.43
					50 ppm Experimental					
18751	1872 6	1065	649	52 (7.5)	76 (11.0)	99 (14.3)	297 (43.0)	32.22	63.60	78.06
					100 ppm Experimental					
18763	1873 5	1065	593	41 (5.9)	79 (11.4)	105 (15.2)	369 (53.5)	35.76	48.65	76.67
18758	1873 6	1065	649	56 (8.1)	83 (12.0)	100 (14.5)	301 (43.6)	31.76	59.55	79.11
					200 ppm Experimental					
18764	1874 5	1065	593	35 (5.1)	66 (9.5)	106 (15.3)	376 (54.5)	32.34	46.40	77.17
18759	1874 6	1065	649	56 (8.1)	84 (12.2)	102 (14.8)	306 (44.3)	32.52	59.90	80.22
					500 ppm Experimental					
18755	1875 4	1065	593	66 (9.6)	94 (13.6)	106 (15.3)	383 (55.5)	35.35	47.20	75.75
18756	1875 6	1065	593	63 (9.2)	93 (13.5)	107 (15.5)	380 (55.1)	33.10	44.10	75.52
18249	1875 C3	1065	593	77 (11.2)	101 (14.6)	113 (16.4)	429 (62.2)	27.51	38.50	70.47
18714	1875 C4	1065/1250	593	47 (6.8)	72 (10.4)	81 (11.7)	452 (65.6)	30.06	32.80	55.88
18985	1875 C5	1093	649	48 (6.9)	75 (10.8)	102 (14.8)	368 (53.5)	27.82	44.60	69.40
					700 ppm Experimental					
18250	1876 B6	1065	593	70 (10.2)	101 (14.7)	117 (17.0)	456 (66.1)	27.20	38.00	66.87
18715	1876 B4	1065/1250	593	44 (6.4)	63 (9.1)	84 (12.2)	470 (68.1)	26.03	30.55	48.76
18986	1876 B5	1093	649	62 (9.0)	89 (12.9)	107 (15.5)	393 (57.0)	27.33	41.25	66.29
					1000 ppm Experimental					
18251	1877 B3	1065	593	65 (9.4)	103 (15.0)	121 (17.5)	449 (65.1)	28.08	36.15	68.95
18987	1877 B4	1065	649	57 (8.2)	93 (13.5)	117 (16.9)	380 (55.1)	28.20	44.65	70.91